

Chapter 2

Potential Storage Materials

A wide range of materials are currently being considered as potential reversible hydrogen storage media. In this chapter we will expand on the material types introduced in [Sect. 1.4](#) and discuss some of their storage properties. We begin with microporous adsorbents, which physisorb molecular hydrogen at low temperatures. Secondly, we look at the interstitial hydrides, which are reactive metals that reversibly absorb dissociated atomic hydrogen into their bulk as an interstitial. We then cover the complex hydrides that bind atomic hydrogen either covalently or ionically and release it via solid state decomposition, and finally consider some alternative storage materials that do not fit readily into the other categories. A summary of some basic hydrogen storage properties of the material types covered in this chapter is given in [Table 2.1](#).

2.1 Microporous Materials

Microporous materials adsorb molecular hydrogen. The narrow width of their micropores leads to an increase in the density of hydrogen in the pore network compared to the gas phase. This occurs primarily at relatively low, sub-ambient, temperatures. According to the current IUPAC classification scheme [\[1\]](#), pores can be divided by size into three categories: *micropores*, of dimensions below 2 nm, *mesopores*, between 2 and 50 nm, and *macropores*, which are greater than 50 nm. The porous materials being considered for physisorbed molecular hydrogen storage are predominantly microporous. They are also often in the subcategory of *ultramicroporous*, in which the pore dimensions are less than 0.7 nm; close to the size of a single hydrogen molecule. At these length scales the adsorption potentials of the opposing pore walls overlap, which significantly increases the density of the adsorbed hydrogen, compared to the gas phase, at any given temperature and pressure.

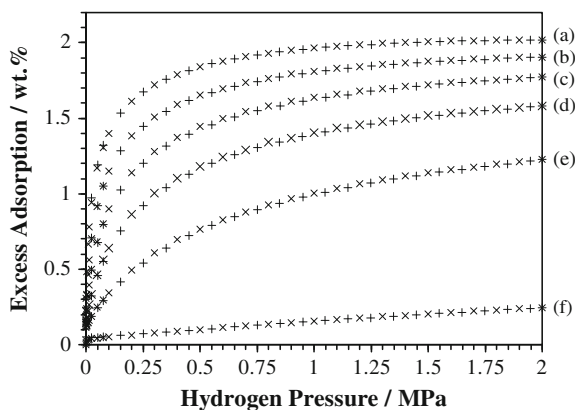
The use of these materials as gas storage media has been considered for a number of years. For example, various reports can be found in the literature that describe the use of microporous carbons, zeolites and other adsorbents to enhance the storage capacity of natural gas (methane) storage tanks [2] and the use of microporous carbons and zeolites for hydrogen storage has been discussed for the past 30 years¹ [5–7]. Recently, however, the level of interest in the use of these materials for hydrogen storage has increased dramatically. The proposal of carbon nanotubes as a possible storage medium first attracted significant attention in the late 1990s and the exciting progress made in the synthesis of new porous hybrid materials [8] has further invigorated the field. Progress continues with the synthesis of microporous organic polymers, as well as new hybrid material classes, and new candidate materials are likely to emerge as the search, as well as the interest in these materials for a range of other applications, continues. In this section we cover the main groups of adsorbents currently being considered as storage media.

Before beginning, however, we will briefly discuss the hydrogen uptake behaviour of microporous materials because it is broadly similar for all the materials considered in this section. According to the conventional classification of adsorption by IUPAC [1, 9], isotherms can be of six general types (I–VI). Hydrogen adsorption by microporous materials invariably corresponds to Type I, which is concave to the pressure axis and saturates at a finite limit. Note that the identification of supercritical hydrogen adsorption as Type I refers to the absolute hydrogen uptake rather than the experimentally determined excess uptake (see Sect. 3.1.1.3). The excess adsorption typically peaks at an elevated pressure and then decreases as the hydrogen gas density increases yet further. This behaviour is typical for high pressure adsorption at supercritical temperatures [10]. The amount of adsorption that occurs at any given pressure decreases with increasing temperature, although the form of the absolute adsorption isotherm will generally remain the same. As an example, Fig. 2.1 shows some hydrogen adsorption data for Na-X zeolite, determined gravimetrically up to a pressure of 2.0 MPa in the temperature range 87–237 K. It can be seen that, as expected for pure physisorption, the adsorption and desorption isotherms show good reversibility, with no observable hysteresis.

The kinetics of hydrogen adsorption by microporous materials are very rapid, which is practically advantageous for hydrogen storage (see Sect. 3.3), but low temperatures are required to achieve significant capacities at useful storage pressures. In practice, low temperature storage requires cooling, which inevitably adds to the weight of a storage unit and is therefore a significant disadvantage. The hydrogen adsorption capacity of microporous materials at ambient temperature is currently too low for practical use [12]. However, the hope is to enhance the interaction of hydrogen with the materials to allow this possibility in the future.

¹ Hydrogen adsorption by porous materials has, however, been studied since the early twentieth century [3, 4].

Fig. 2.1 Hydrogen adsorption (+) and desorption (×) isotherms for Na-X zeolite at a number of sub-ambient temperatures. The isotherms were measured gravimetrically at the following temperatures: (a) 87 K, (b) 97 K, (c) 107 K, (d) 117 K, (e) 137 K and (f) 237 K. Reproduced from Broom et al. [11] with permission from Hiden Isochema Ltd



Another drawback is their volumetric storage capacity, an issue that has occasionally been sidelined in favour of gravimetric considerations. In order to achieve high volumetric capacities, adsorbed hydrogen must be stored at relatively high densities within the pores and the microporous framework should also occupy a low proportion of the geometric volume of the material.²

2.1.1 Carbons

Several types of microporous carbons have attracted interest for hydrogen storage, including activated carbons, carbon nanotubes and nanofibres and, more recently, microporous templated carbons [13]. Carbon is very attractive technically as a host because of its low molar mass. It is also chemically stable and can be synthesised in a number of different forms. From a practical point of view, porous carbons are already commercially produced in large quantities for a broad range of applications and are relatively inexpensive.

2.1.1.1 Activated Carbon

Activated carbon is a porous form of carbon that can be synthesised via both chemical or physical activation methods. Depending on both the raw material and the activation method and conditions, the resultant carbon will have a specific, although not necessarily clearly defined, pore structure. Activated carbons can be predominantly macro, meso or microporous, but the latter are the main focus for hydrogen storage. Activated carbons tend to have slit-shaped pores [14, 15], but

² The definition of the geometric volume is the volume occupied by the sample including both closed and open pores (see the definition of geometric density in Sect. 6.2.1).

also exhibit a relatively wide pore size distribution. This is in contrast to the crystalline adsorbents, such as the zeolites or Metal-Organic Framework (MOF) materials covered in the following sections, which have a well defined pore size and pore geometry. There have been many studies of hydrogen adsorption by activated carbons and, according to Yürüm et al. [13], these show that gravimetric storage capacities can reach 5.5 wt% at 77 K. However, the pore structure of carbons can take many different forms, depending on the chosen activation method and the raw material used for the synthesis, and so a range of capacities have been reported in the literature. Carbons are also challenging to characterise accurately, as demonstrated by the variability in the results of a recent interlaboratory study [16], which will be discussed in more detail in the closing chapter of this book.

In addition to the experimental characterisation difficulties, modelling work on these materials is significantly limited by the lack of knowledge regarding their microstructure, which is fundamentally different to crystalline microporous adsorbents. The latter can be characterised crystallographically using powder diffraction (Sect. 5.3) but activated carbons are X-ray and neutron amorphous. The structure itself therefore has to be modelled, or an idealised slit-pore model used. However, estimated maximum theoretical capacities appear to agree reasonably well with those determined experimentally.

Jordá-Beneyto et al. [17] advocate the use of activated carbon monoliths for hydrogen storage because microporous activated carbon in this form has a greater bulk density than the same carbon in powder form. Equivalent monoliths formed from MOFs have not yet been reported in the literature, at the time of writing, and it is possible that activated carbon monoliths have significant advantages in terms of volumetric storage capacity. An experimental comparison would be worthwhile, however, because it may show that the higher gravimetric capacities reported for the best performing MOFs (see Sect. 2.1.3) are counterbalanced by lower practical volumetric capacities in real storage devices due to lower bulk material density.

2.1.1.2 Carbon Nanotubes and Other Carbon Nanostructures

The hydrogen sorption properties of carbon nanostructures, such as nanotubes and nanofibres, have been investigated extensively in recent years. As described briefly in Chap. 1, there has been considerable controversy over the storage properties of some of these materials since the publication of the first report of the potential for room temperature storage of hydrogen by carbon nanotubes [18]. Carbon nanotubes are cylindrical nanostructures formed from rolls of graphene. They can have diameters of 0.7 nm up to several nanometres and form single and multi-walled tubes that form close-packed bundles [19]. In 1997, Dillon et al. [18] reported potential room temperature storage capacities of 5–10 wt%, a figure derived from a rather optimistic extrapolation of thermal desorption data measured on a sample consisting of an estimated 0.1–0.2 wt% of nanotubes (the remainder of the sample was uncharacterised soot). The high temperature desorption peak claimed by Dillon et al. [18] to indicate the ambient temperature storage capabilities of the

nanotube sample was later shown by Hirscher et al. [20] to be due to metal nanoparticles deposited during an ultrasonic purification process [19] (see Sect. 6.2). Although modelling work has predicted the possibility of relatively high storage capacities in nanotube structures the reported values are no greater than those for activated carbons and it therefore appears that they offer no significant advantage over other forms of carbon, which can be considerably easier to synthesise in large quantities.

Carbon nanofibres consist of graphene layers, stacked together in various orientations with respect to the axis of the fibre, including parallel and perpendicular, as well as intermediately angled (so-called *herringbone*) configurations. In 1998, Chambers et al. [21] reported incredibly high capacities for carbon nanofibres of up to 67 wt%. Questionable experimental procedures in this work that produced anomalous hydrogen storage capacities for well known and understood hydrides, together with the unphysical nature of the claimed capacity, which corresponds to a H/C atomic ratio of around 24, indicated that the measured capacities were significantly overestimated. Subsequent studies of both nanotubes and nanofibres produced a wide range of values, none of which substantiated these initial claims, and an interesting controversy developed. Tabulated values can be found in a number of articles, showing the spread of the data found in the literature at the time [13, 22, 23]. Although the issue has not yet been resolved completely, it seems fairly safe to conclude that both nanotubes and nanofibres are unlikely to be the hydrogen storage panacea that some authors have suggested. In addition to nanotubes and nanofibres, fullerenes and carbon nanohorns have also been investigated, either experimentally or theoretically, for their hydrogen storage properties [24, 25].

2.1.1.3 Templated Carbons

Templated carbons are a form of microporous or mesoporous carbon typically synthesised by introducing a carbon precursor, such as sucrose or acetonitrile, into the pores of an inorganic template. Carbonisation and the subsequent removal of the template results in a pore structure that is relatively well defined compared to their activated carbon counterparts [26, 27]. There have been a number of studies on these materials and they can exhibit impressive hydrogen adsorption properties, with the largest capacity reported to date being 6.9 wt% for a zeolite-templated carbon at 77 K and 20 bar [12, 26]. The uptake was Type I, with an estimated saturation capacity of 8.33 wt%. Unlike activated carbons, these materials show evidence of microstructural ordering through the appearance of Bragg peaks in their X-ray powder diffraction patterns. Another type of templating uses carbide precursors and can produce microporous carbons with very well defined pores sizes [28, 29]. According to Gogotsi et al. [29] the hydrogen uptake of these so-called *Carbide-Derived Carbons* (CDCs) can reach 4.7 wt% at 60 bar and 77 K. Although this is not particularly high, the CDCs offer the opportunity to further

tune and optimise the pore size and continued investigation of the interaction of hydrogen with these materials would undoubtedly be valuable.

2.1.2 Zeolites

Zeolites are microporous aluminosilicates formed from AlO_4 and SiO_4 tetrahedra. They have a range of practical applications that exploit their ion exchange, molecular sieving and catalytic properties. The term *zeolite* is often used to describe compounds with similar structures that are formed by elements other than Al and Si, including P, Ga, Ge, B and Be, but these materials are also known as *zeotypes*. These materials form a variety of different crystallographic structures.³ Their ordered crystalline nature gives them uniform cavities and channels with dimensions in the microporous regime. The framework structures are relatively rigid and, as with all microporous solids, they have high specific surface areas and large pore volumes. Their properties can be tuned by altering the Si/Al ratio of the framework, or the equivalent stoichiometry in the case of zeotypes, with limits in the range $0.5 < \text{Si/Al} < \infty$. The anionic nature of zeolite frameworks leads to the presence of cations within their structure. Exchange of these cations can also significantly alter their properties.

Although zeolites are highly porous, with high surface areas, the hydrogen storage capacities reported in the literature have, to date, been fairly low. In their study of low pressure (< 0.1 MPa) hydrogen uptake by a range of porous solids, Nijkamp et al. [31] concluded that zeolites are less likely to be effective as hydrogen storage materials, in comparison to porous carbons, due to their limited pore volume. Vitillo et al. [32] tabulated a number of the experimentally determined hydrogen uptakes, with the highest reported uptake at 77 K or above being 1.81 wt%, as reported by Langmi et al. [33]. This figure was found for Na-Y zeolite at a pressure of 1.5 MPa. According to Anderson [34], the highest reported uptake until recently was 2.55 wt% for Na-X at 77 K and 40 bar (4.0 MPa) [35].

The results of the molecular mechanics simulations performed by Vitillo et al. [32] predict that the maximum storage capacities for a range of zeolites are in the region of 2.65 and 2.86 wt%, whereas van den Berg et al. [36] found that, theoretically, the hydrogen content could reach (4.8 ± 0.5) wt% for sodalite (SOD) structures.⁴ In the study by Vitillo et al. [32] a lower figure of 1.92 wt% was determined for SOD. In later work, van den Berg et al. [37] found lower values for the saturation uptake using Grand Canonical Monte Carlo (GCMC) simulations, although the higher figures are supported by Song and No [38], who found an

³ 176 different structure types are listed by Baeloche et al. [30].

⁴ Van den Berg et al. [36] and Vitillo et al. [32] both calculated the maximum hydrogen uptake using molecular mechanics simulations but used different convergence criteria to define when the hydrogen capacity had reached saturation. In addition, the latter study included a correction for the zero point motion of hydrogen, whereas the former did not.

uptake of 4.45 wt% for Mg-X. However, even these higher capacities are low in comparison to the challenging US DOE storage system targets.

The temperature dependence of hydrogen adsorption by Na-X zeolite is illustrated in Fig. 2.1. These isotherms were measured gravimetrically up to a pressure of 2 MPa in the temperature range 87–237 K. At room temperature and moderate pressure, hydrogen uptake by zeolites is low. Hydrogen storage at higher temperatures has been proposed through the mechanism of *encapsulation* [39–41], a process by which, in the case of zeolites A, X and Y, hydrogen molecules enter the sodalite cages. However, this does not appear to be a mechanism capable of delivering practical storage capacities.⁵

Enthalpies of adsorption, a measure of the strength of the hydrogen-adsorbent interaction (see Sect. 3.2.1), for zeolites can have a range of values. Garrone et al. [42] report $-\Delta H^0$ (standard adsorption enthalpy) values in the range 3.5–18 kJ mol⁻¹, with the largest of these values being found for (Mg, Na)-Y zeolite [43]. These values were determined using infrared spectroscopy (see Sect. 5.4.3).

Zeolites have a number of significant practical advantages over other microporous adsorbents. They possess high thermal stability in comparison to metal-organic frameworks and organic polymers, for example. Thorough degassing of the framework can therefore be performed at 350°C (623 K) with no decomposition. Their crystalline nature allows easy characterisation of the host material and they have a well defined and understood pore size in comparison with activated carbon. Current industrial production of synthetic zeolites also demonstrates the feasibility of their synthesis in large quantities, although this is also the case for carbons. However, it seems unlikely that zeolites will be useful as practical hydrogen storage media for onboard applications. Felderhoff et al. [44] support this view and argue that they do not show the required capacities for practical storage applications. Zeolites are, however, certainly valuable as model systems for the further investigation of the interaction of hydrogen with microporous materials [45], and so their continued study is both likely and worthwhile. Anderson [34] covered hydrogen storage in zeolites in detail and this review is recommended to interested readers.

2.1.3 Metal-Organic Frameworks

Metal-Organic Frameworks (MOFs) are crystalline inorganic-organic hybrid solids consisting of metal ions or clusters linked by organic bridges [8, 46, 47]. The archetypal MOF is Zn₄O(bdc), where bdc = 1,4-benzenedicarboxylate, which

⁵ Hydrogen encapsulation has been investigated by a number of authors [39–41] by loading zeolites at elevated temperatures under a hydrogen atmosphere, then cooling the sample to ambient and performing TPD up to temperatures of 673 K to desorb the encapsulated hydrogen. However, storage capacities were found to be low; for example, 0.6 wt% for Na-X at hydrogenation pressures of 13.3 kpsi (91.7 MPa) [39].

is commonly known as either MOF-5 or IRMOF-1.⁶ This material consists of zinc oxide clusters joined by benzene linkers. The metallic clusters are known generically as Secondary Building Units (SBUs) and in MOF-5 the structure forms a highly porous cubic network. A number of reviews specifically addressing the storage of hydrogen using MOFs can be found in the literature and these are recommended to interested readers [12, 48–52]. Hundreds of different MOFs have been studied for their hydrogen adsorption properties. Murray et al. [52], for example, list hydrogen uptake data⁷ for 177 different MOFs and the current level of interest in these materials is such that since this recent review the amount of data in the literature is likely to have grown considerably.

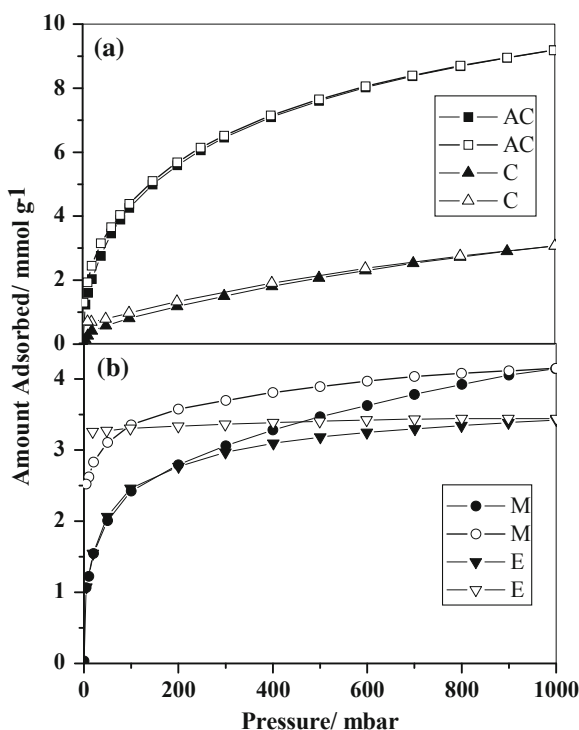
Hydrogen storage by metal-organic frameworks was first reported by Rosi et al. [53] in a study including MOF-5, IRMOF-6 and IRMOF-8. Their initial claimed capacity for MOF-5 of 4.5 wt% at 77 K and 0.07 MPa met with some scepticism [54], and was subsequently reduced in a later report [55]. Nevertheless, following their discovery there have been many more studies on hydrogen storage by other framework materials and the erroneously high capacity claimed for low pressure adsorption has since been exceeded at higher pressures. Tabulated data compiled by Collins and Zhou [49] and Thomas [12] indicate maximum hydrogen uptakes at 77 K of between approximately 1.0 and 7.5 wt% for a range of MOFs. The highest value of 7.5 wt% was found for MOF-177 [Zn₄O(btb), where btb = 1,3,5-benzenetribenzoate], as reported by Yaghi et al. [55, 56]. This uptake was found at a measurement pressure of 7.0 MPa; the uptake at 0.1 MPa was 1.25 wt%. The highest reported value at room temperature (298 K) is 1.4 wt% reported for a pressure of 9.0 MPa, for Mn(btt), where btt = 1,3,5-benzenetristetrazolate, by Dincă et al. [57]. This MOF also adsorbs 6.9 wt% at 77 K and a hydrogen pressure of 9.0 MPa.

Aside from the large number of possible combinations of different SBUs and organic linkers, and hence possible pore geometries, the presence within the frameworks' pores of *exposed metal sites* is another reason for the interest in MOFs. To either increase the operating temperature of a microporous hydrogen store, or increase the maximum storage capacity at near ambient temperature, an increase in the strength of the hydrogen-surface interaction is required. Molecular hydrogen is known to form so-called *Kubas complexes* with nearly all transition metals [58] and the possibility of enhancing the hydrogen-surface interaction through a similar mechanism offers the promise of developing MOFs with much improved storage properties. This aspect of hydrogen adsorption in MOFs was the

⁶ Metal-organic frameworks tend to be known by the initials assigned to them by the researchers responsible for the original synthesis. These initials do not follow any particular pattern but tend to refer to either the material type or the researchers' institution. Examples include MOF (Metal-Organic Framework), MIL (Materials of Institute Lavoisier), IRMOF (IsoReticular Metal-Organic Framework) and UCM (University of Michigan Crystalline Material).

⁷ Note that the majority of the data reports the hydrogen uptake at atmospheric pressure, which gives limited information with regard to the reversible capacity for storage purposes (Sect. 3.1.1), and therefore further studies at elevated pressures are required.

Fig. 2.2 Hydrogen adsorption and desorption isotherms measured at 77 K for an activated carbon (AC), and three metal-organic frameworks (C, M and E). Two of the MOFs (M and E) exhibit hysteretic hydrogen adsorption behaviour, whereas the activated carbon and MOF C exhibit conventional reversible Type I adsorption behaviour. From Zhao et al. [60]. Reprinted with permission from AAAS



focus of the review by Dincă and Long [51], and was also addressed recently by Hoang and Antonelli [59].

Another interesting feature is *framework flexibility*. In 2004, Zhao et al. [60] reported two MOFs that showed hysteretic hydrogen adsorption, due to structural flexibility, so that for a given temperature the materials desorbed hydrogen at a significantly higher pressure than that of adsorption. The hysteresis is shown in Fig. 2.2, which includes isotherm data illustrating the hysteresis in comparison with an activated carbon and a MOF exhibiting conventional reversible Type I behaviour. The hysteresis is unusual for molecular hydrogen physisorption, which is normally fully reversible at any given temperature. Thomas [12] gives a number of examples of MOF materials that show flexibility during the adsorption and desorption of guest molecules, either with or without the breaking of chemical bonds in their structure. The flexibility can lead to structural transformations that involve stretching, rotational, breathing and scissoring mechanisms. The review on framework flexibility by Fletcher et al. [61] is recommended to interested readers.

Many studies have focused on the enthalpy of hydrogen adsorption for MOFs, since this is a measure of the strength of interaction between hydrogen and the surface or pore structure (see Sect. 3.2.1). Reported values of the isosteric enthalpy

of adsorption are in the range from 3.8 kJ mol^{-1} for MOF-5/IRMOF-1 [62] to 12.3 kJ mol^{-1} for a mixed zinc/copper metal-organic framework, M'MOF 1 [63].⁸

MOFs hold greater promise as potential storage media than zeolites, as the reported gravimetric capacities are significantly higher and the unique features, such as structural flexibility and exposed metal sites, give them more potential for future development. However, these materials tend to be less robust than zeolites and microporous carbons, because they exhibit lower thermal stability. Nevertheless, their commercialisation is already underway, principally by BASF who market a series of framework materials under the tradename BasoliteTM, and so the practical application and use of these materials on an industrial scale is clearly feasible.

2.1.4 Organic Polymers

There are three main classes of microporous organic polymer that have emerged recently as potential candidates for adsorptive hydrogen storage: *Polymers of Intrinsic Microporosity* (PIMs), *Hypercrosslinked Polymers* (HCPs) and *Covalent Organic Frameworks* (COFs) [64]. The latter are crystalline organic analogues of MOFs, while both PIMs and HCPs are non-crystalline (X-ray and neutron amorphous) materials that have a disordered structure that more closely resembles activated carbon than crystalline materials such as zeolites, MOFs and COFs.

PIMs are rigid and contorted macromolecules that consist of fused-ring components. They form a microporous network as they are unable to pack space efficiently and, as a consequence, have high BET surface areas in the range $500\text{--}1100 \text{ m}^2 \text{ g}^{-1}$ [65, 66]. HCPs derive a similarly high degree of microporosity, and hence high BET surface areas, from a high density of crosslinks, the covalent chemical bonds that occur between macromolecules in polymeric materials [67, 68]. COFs, meanwhile, are crystalline networks formed exclusively from the light elements H, B, C, O and Si, that are linked by strong covalent bonds (B–O, C–O, C–C, B–C, and Si–C) [69, 70].

Hydrogen capacities of up to 2.7 wt%, at 1.0 MPa and 77 K, have been reported for a triptycene-based polymer (trip-PIM) [66]. The reported capacities for HCPs are higher, reaching 3.68 wt% at 1.5 MPa and 77 K for a polymer based on BCMBP [4,4'-bis(chloromethyl)-1,1'-biphenyl] [68]. Although the uptakes of these amorphous organic polymers are not outstanding, they are attractive as potential storage media due to the light elements from which they are formed, and further development and the synthesis of new materials may yet produce a high storage capacity polymer. One disadvantage in comparison to other microporous media is their relatively low thermal stability, which means that care must be taken not to induce thermal decomposition during the degassing process (see Sect. 6.4.1).

⁸ M'MOF 1 is $\text{Zn}_3(\text{bdc})_3[\text{Cu}(\text{pyen})]$, where $\text{pyenH}_2 = 5\text{-methyl-4-oxo-1,4-dihydro-pyridine-3-carbaldehyde}$.

Compared to the relatively conservative capacities reported so far for PIMs and HCPs, the predicted and measured gravimetric capacities of COFs are impressive. Furukawa and Yaghi [70] reported experimental uptakes of 72.4 mg g^{-1} and 70.5 mg g^{-1} for COF-102 and COF-103, respectively. These measurements were made gravimetrically at 77 K and at pressures of up to around 9 MPa. COF-102 and COF-103 are prepared by self-condensation reactions of *tetra*(4-dihydroxyborylphenyl)methane (TBPM) and its silane analogue (TBPS) [71]. Simulated total uptakes reported by Han et al. [69] for COF-105 and COF-108 both exceed 18 wt% at 10.0 MPa and 77 K, with values of 18.3 and 18.9 wt%, respectively. However, these two materials have large free volumes and the volumetric capacity is lower than that of COF-102, which shows a lower simulated and experimental gravimetric capacity.

With regard to the enthalpy of adsorption for hydrogen on organic polymers, Spoto et al. [72] determined a value of approximately $4 \text{ kJ mol}^{-1} \text{ H}_2$ for a HCP (cross-linked poly(styrene-*co*-divinylbenzene) polymer) using infrared spectroscopy (see Sect. 5.4.3). Wood et al. [68], however, determined higher values in the range $6\text{--}7.5 \text{ kJ mol}^{-1} \text{ H}_2$ for the isosteric enthalpies of adsorption from hydrogen isotherms measured at 77 and 87 K. These higher figures were in general agreement with those obtained from accompanying simulations. Measured isosteric enthalpies of adsorption for COFs have been found to be in the range $4\text{--}7 \text{ kJ mol}^{-1} \text{ H}_2$ [70]. The materials that exhibit the largest gravimetric uptake possess the lowest enthalpy of adsorption, perhaps reflecting the fact that larger pore volumes and pore dimensions lead to higher overall hydrogen uptakes, but a concomitant decrease in adsorption potential due to the increased pore dimension.

In addition to PIMs, HCPs and COFs, the hydrogen adsorption behaviour of a number of other organic polymers have been reported in the literature, including dipeptide-based materials [73] and 3,3',4,4'-tetra(trimethylsilylethynyl)biphenyl, a type of organic zeolite [74], although the uptakes of these materials are relatively modest. Early results indicating high hydrogen uptake by HCL-treated conducting polymers, polyaniline and polypyrrole, were not successfully reproduced by other investigators [75]. Another new group of materials reported by Rose et al. [76] are *Element Organic Frameworks* (EOFs). These authors reported hydrogen uptake in two of these materials, poly(1,4-phenylene)silane (EOF-1) and poly(4,4'-biphenylene)silane (EOF-2), of 0.94 and 1.21 wt%, respectively, at 77 K and 0.1 MPa. Although, to date, none of these compounds have been proven as a practical storage material, it is likely that significant further progress will be made as synthetic chemists continue to discover interesting new microporous media. Further study will also undoubtedly improve our understanding of the interaction of hydrogen with organic microporous materials.

2.2 Interstitial Hydrides

These are formed from metallic elements or compounds that react with gaseous hydrogen to produce binary, or higher, hydrides. Molecular hydrogen dissociates

into atomic hydrogen on the surface of the host material and enters the bulk via diffusion between interstitial sites in the host lattice. Most elemental metals will absorb hydrogen in this manner under certain conditions of temperature and hydrogen pressure; however, binary hydrides (MH_x , where M is a metallic element and x is the hydride stoichiometry) are generally either too unstable or too stable for use as practical storage materials. The former means that the pressures at which the host reversibly absorbs and releases hydrogen are too high at practical storage temperatures, and the latter means the pressures are too low. In terms of formation or decomposition enthalpies (see Sect. 3.2.2), ΔH is too high in the former case (either small negative numbers or positive) and too low in the latter (a relatively large negative value). However, when two or more metallic elements are combined, particularly one that forms a stable hydride and one that does not, the resultant alloy or intermetallic tends to form a hydride of intermediate stability.

The study of metallic hydrides began nearly 150 years ago with the discovery of the hydrogen-absorbing properties of palladium by Thomas Graham [77]. Work beginning in the 1960s resulted in the later commercialisation of Nickel-Metal Hydride (Ni-MH) batteries in which the negative electrode material forms an intermetallic hydride. Although this has been the most commercially successful application of interstitial hydrides, metal hydride technology is also exploited in a number of other application areas, including gas separation and purification, temperature sensing, thermal compression, and refrigeration or cryocooling [78–80]. For mobile storage applications, the gravimetric capacity of many interstitial hydrides is relatively low, but some of these compounds show remarkable and practical hydrogen absorption and desorption characteristics, and they are likely to play an important role in a future hydrogen economy. A thorough account of the physics of interstitial hydrides, along with many of their basic properties, can be found in the monograph by Fukai [81] and this is recommended to interested readers. Further extensive coverage can be found in the volumes edited by Alefeld and Völkl [82, 83], Schlapbach [84, 85] and Wipf [86].

In this section, we look at a number of the different types of interstitial hydride, and cover intermetallic compounds, solid solution alloys, modified binary hydrides, and amorphous and nanostructured hydrides, including mechanically milled materials, amorphous alloys produced using other methods, and quasicrystals.

2.2.1 Intermetallic Compounds

The host materials in this group are ordered stoichiometric compounds typically formed from two metallic components, A and B. The A and B components tend to form hydrides AH_x and BH_y , with enthalpies of formation ΔH_A and ΔH_B , representing a stable and an unstable hydride, respectively. As mentioned above, the resultant intermetallic hydride $\text{A}_m\text{B}_n\text{H}_z$, where m and n are integers and z is a real number, will then tend to have an enthalpy of formation, ΔH_{AB} , where $\Delta H_A < \Delta H_{AB} < \Delta H_B$. Varying the ratio n/m then shifts the value of ΔH_{AB} in either

direction. The components A and B can generally be fully or partially substituted by other elements of relatively similar size or chemistry. Hydrogen-absorbing intermetallics form a number of different groups, which can be distinguished by their stoichiometries, including AB_5 , A_2B_7 , AB_3 , AB_2 , AB and A_2B compounds [54, 87]. Early reports of the reversible hydriding properties of intermetallic compounds include those by Libowitz et al. [88], published in 1958, on $ZrNiH_3$ and the early work of Reilly and Wiswall [89, 90] in the late 1960s on the hydrogenation of Mg_2Ni and Mg_2Cu . These reports pre-date the discovery of the reversible hydrogenation of $LaNi_5$ around 1970 [91] and the subsequent increase in the amount of metal hydride research that ultimately led to the commercialisation of Ni-MH battery technology, and the research into metal hydride-based hydrogen storage that continues today.

A vast number of A and B element combinations are now known to form reversible hydrides, although relatively few do so at useful temperatures and pressures. Calculated ΔH values for 1265 different A_5BH_x , A_2BH_x , ABH_x , AB_2H_x and AB_5H_x intermetallic hydrides, along with measured values for 63 binary hydrides and 135 ternary hydrides, were tabulated by Griessen and Riesterer [92]. Similarly, Buschow et al. [93] provide tabulated data and references on a large number of compounds, including studies using many of the complementary techniques we introduce in Chap. 5. In this section we will cover some of the combinations and stoichiometries that are of practical interest for hydrogen storage. Note that different stoichiometries can often be found within the binary phase diagram of any given pair of constituents but, because of the dramatic effect that the ratio of elements has on the hydriding properties, it is likely that only one of these has a formation enthalpy that gives the material hydrogen absorption and desorption capabilities in a practical temperature and pressure regime. As an example, let us consider La and Ni, which combine to produce the well known hydride-forming compound $LaNi_5$. La forms a very stable hydride, LaH_2 , with $\Delta H = -104 \text{ kJ mol}^{-1} \text{ H}$, while Ni forms a very unstable hydride ($\Delta H = -3 \text{ kJ mol}^{-1} \text{ H}$) [92]. The calculated values of Griessen and Riesterer [92] for the La–Ni–H system are -13.3 , -23.0 , -40.3 , -60.6 and $-82.5 \text{ kJ mol}^{-1} \text{ H}$ for $LaNi_5$, $LaNi_2$, $LaNi$, La_2Ni and La_5Ni , respectively. Although these values do not match the experimental values particularly well,⁹ the dependence on the ratio of the two constituent metal elements can be seen clearly and matches the trend observed experimentally: the lower the Ni content of the host intermetallic, the more stable the associated hydride compound.

Some intermetallics, principally Mg-based compounds such as Mg_2Ni and Mg_2Cu , form stoichiometric hydride complexes upon hydrogenation and can therefore be categorised as complex transition metal hydrides rather than

⁹ The calculated values were obtained using the semi-empirical band structure model of Griessen and Driessen [94]. The discrepancy between these values and experiment most likely originates from the implicit assumption in this model that each hydrogen atom sits in the same environment, surrounded by an average number of A and B atoms, rather than on crystallographically distinct interstitial sites.

interstitial intermetallic hydrides. Furthermore, there are interesting cases, such as the intermetallic compound LaMg_2Ni that forms a mixed hydride ($\text{LaMg}_2\text{NiH}_7$) consisting of NiH_4 tetrahedra and ‘interstitial’ H^- ions, which blur the boundary between the interstitial intermetallic hydrides and their complex counterparts, which are covered in Sect. 2.3 [95]. To add to the already slightly fuzzy picture, many of the intermetallics can be under or over-stoichiometric. The distinction between the intermetallics and solid solution alloys (Sect. 2.2.2) still exists, however, because the A and B components of an intermetallic tend to occupy different lattice sites rather than randomly occupying all sites throughout the host lattice. In each of the following sections we will briefly summarise the main groups of interstitial hydride-forming intermetallics that are of interest for hydrogen storage, and we therefore cover AB_5 , AB_2 and AB compounds. We will cover some of the A_2B compounds in Sect. 2.3.4.

2.2.1.1 AB_5 Compounds

The archetypal AB_5 intermetallic is LaNi_5 . This compound readily forms a hydride under fairly moderate hydrogen pressures and ambient temperatures. It has an enthalpy of formation of $-15.7 \text{ kJ mol}^{-1} \text{ H}$ and an enthalpy of decomposition of $-15.1 \text{ kJ mol}^{-1} \text{ H}$ [96]. Hydrogen capacity exceeds LaNi_5H_6 , giving a reversible gravimetric capacity in the region of 1.25 wt% [87]. LaNi_5 and some other binary AB_5 compounds, such as CaNi_5 , can be subject to significant disproportionation and therefore lose their reversible capacity during hydrogen cycling (see Sect. 3.1.2). However, these compounds can be modified via partial substitution to reduce the disproportionation. The most effective substituent for this purpose for LaNi_5 is Sn, with a composition of $\text{LaNi}_{5-x}\text{Sn}_x$, where $x \approx 0.2$ [97]. For economic reasons, mischmetal (Mm), a naturally occurring mixture of rare earths, can be substituted for the La as the A component. As well as the LaNi_5 , $\text{LaNi}_{5-x}\text{Sn}_x$ MmNi_5 and CaNi_5 intermetallics, hydride-forming AB_5 compounds can be composed of many other elemental combinations, with the A elements tending to be either one or more of the lanthanides or Ca, as in the compounds mentioned above, or Y and Zr, and the B elements any of a range of elements including Co, Al, Mn, Fe, Cu, Sn, Si and Ti, as either full or partial constituents [87, 98]. The hydrogen capacities, plateau pressures and the enthalpies of hydride formation of 36 binary, ternary and quaternary AB_5 compounds were tabulated by Ivey and Northwood [99] and 477 records for AB_5 compounds are currently listed in the Sandia National Laboratories (US) Metal Hydride Properties database¹⁰ [100].

It can be seen clearly that the gravimetric storage capacity of these materials is substantially lower than the current US DOE target for mobile hydrogen storage applications. However, the AB_5 -based intermetallics show some remarkable cycling properties including excellent resistance to gaseous impurity contamination, good long term cycling stability and a high volumetric storage density, and

¹⁰ <http://hydpark.ca.sandia.gov/DBFrame.html>, accessed 2nd January 2010.

are therefore a prime example of a practically effective reversible hydrogen storage material.

2.2.1.2 AB₂ Compounds

AB₂ compounds can be formed from the combination of many different elements. According to Sandrock [87], the A elements are typically from group 4 (Ti, Zr, Hf) or the lanthanoids (La, Ce, Pr, and so forth), whereas the B element can be a transition or non-transition metal, with a preference for V, Cr, Mn and Fe. Feng et al. [101] summarise the elements of interest for electrochemical applications of AB₂ compounds as A = Mg, Zr and Ti, and B = V, Cr, Mn and Ni, although many more can be used as partial substituents. The Sandia database¹⁰ currently includes 625 records for AB₂ compounds.

These intermetallics crystallise in either the hexagonal C14 or cubic C15 Laves phase structure. Like the AB₅ compounds, they can show a range of hydriding properties depending on the elemental composition. This allows the hydriding properties of a given AB₂ material to be tuned via partial elemental substitution. A number of examples of multicomponent AB₂ compounds can be found in Young et al. [102], a recent report on Ti_xZr_{1-x}(VNiCrMnCoAl)₂, a C14 Laves phase AB₂ proposed for use as a battery electrode material. In addition to partially substituted compounds, sub- or superstoichiometric compositions can also be formed. This modification also affects the hydriding properties of a material [79]. Bowman and Fultz [79] gave a good example of the effects of non-stoichiometry using the Zr–Mn–H system. Substoichiometric ZrMn_{2-x}, where x is positive, has a lower plateau pressure and a significantly lower reversible hydrogen storage capacity than ZrMn₂, whereas superstoichiometric ZrMn_{2+x} has a higher plateau pressure and only a slightly smaller reversible capacity than the stoichiometric compound [79, 103].

AB₂ intermetallics have been used practically as reversible hydrogen storage materials. In the 1980s, a fleet of Daimler vans and automobiles were operated using AB₂-based hydrogen stores containing the non-stoichiometric compound Ti_{0.98}Zr_{0.02}Cr_{0.05}V_{0.43}Fe_{0.09}Mn_{1.5} [104]. This intermetallic exhibits very fast kinetics and good long term cycling stability (see Sect. 3.1.2) [79]. On the other hand, high material costs and a gravimetric storage capacity of 1.8 wt% do not, in view of the current US DOE targets, make it particularly practical for widespread use. However, despite this it is another example, along with the AB₅-based compounds, of a conventional interstitial metallic hydride that works well in real applications by satisfying many of the required performance criteria.

2.2.1.3 AB Compounds

In comparison to the number of different AB₂ and AB₅ compositions reported in the literature, the number of AB compounds of interest for hydrogen storage is

fairly limited. The earliest study of an intermetallic hydride, by Libowitz et al. [88], featured an ABH_x intermetallic hydride, ZrNiH_3 , and many other metallic AB compounds form hydrides; 179 records are currently listed in the Sandia database.¹⁰ However, it is only TiFe that is of practical interest for storage applications. The hydrogen-absorbing properties of this compound were originally discovered by Reilly and Wiswall around 1970 [105].¹¹ It achieves a total gravimetric capacity of 1.86 wt% at $H/M = 0.975$, with a reversible capacity of 1.5 wt% [87]. There have been many studies on the hydrogen absorption properties of TiFe and it has reversible hydrogen storage characteristics in a useable range. It has an ordered Body-Centered Cubic (BCC) structure, and shows two distinct plateaus in its hydrogen absorption isotherm. Partial substitution can again be used to modify the hydrogen absorption behaviour. Examples include the partial substitution of Fe with Mn and Ni, which lower the pressure of the first ambient temperature isotherm plateau, and therefore stabilise the hydride with respect to pure TiFe. TiFe and $\text{TiFe}_{0.85}\text{Mn}_{0.15}$ show good long term cycling stability, they are low cost, and tend not to be pyrophoric [87], unlike the AB_5 compounds. Unfortunately their activation is relatively difficult and they are significantly more sensitive to gaseous impurities than AB_5 intermetallics. As with most of the intermetallic hydrogen storage compounds, their gravimetric capacities are low in comparison to the current US DOE targets, but they are nonetheless favourable to many other interstitial hydrides.

2.2.2 Solid Solution Alloys

Solid solution alloys formed by dissolving one or more hydrogen-absorbing metallic elements in another also show interesting hydrogen storage properties. Unlike the intermetallics described above, these materials do not necessarily have stoichiometric or near-stoichiometric compositions. They can be formed from a number of host solvents, including Pd, Ti, Zr and V; thermodynamic data for many solid solution alloy hydride compositions are given by Fukai [81]. From a hydrogen storage point of view, Pd-based alloys suffer from low gravimetric capacities and the high cost of palladium, and Ti and Zr-based solid solutions tend to be too stable. However, vanadium-based alloys have been found to possess favourable absorption properties, and distinct advantages in terms of gravimetric capacities over some intermetallics. Although pure vanadium is prohibitively expensive, the use of low cost ferrovanadium has shown promise and so Fe-containing V-based solid solution alloys make feasible hydrogen storage materials [87].

¹¹ Results had been presented at symposia 4 to 5 years prior to the report published in 1974 [105].

Tabulated data presented by Sakintuna et al. [106] indicate that typical gravimetric hydrogen capacities can approach 4 wt% for Ti–V–Fe ($\text{Ti}_{43.5}\text{V}_{49.0}\text{Fe}_{7.5}$) and Ti–V–Cr–Mn alloys, although the latter requires elevated temperatures in the range 520–745 K. The pressure-composition isotherms for these materials show two plateaus, of which only the higher pressure plateau region can be exploited for hydrogen storage applications. Therefore, in a practical pressure range, the reversible capacity is significantly lower than the maximum capacity quoted above at around 2.5 wt%. In their study of Ti–V–Fe alloys, Nomura and Akiba [107] defined the “Available Hydrogen Quantity” (AHQ) as being the difference between the hydrogen content at 100 kPa on the absorption and desorption isotherms at 253 and 573 K, respectively. They found the AHQ to be 2.4 wt% for $\text{Ti}_{43.5}\text{V}_{49.0}\text{Fe}_{7.5}$. Cho et al. [108], meanwhile, reported a reversible capacity of 2.3 wt% for $\text{Ti}_{0.32}\text{Cr}_{0.43}\text{V}_{0.25}$; they also found that the alloy exhibits good cyclic stability, maintaining a reversible capacity of approximately 2 wt% over the course of 1000 hydriding and dehydriding cycles.

Many different compositional variations of the solid solution alloys can be found in the literature [108–112]. The so-called Laves phase-related BCC solid solution alloys are related materials, which are Ti–V–Mn, Ti–V–Cr and Ti–V–Cr–Mn compounds that contain both Laves and BCC phases. The hydrogen storage properties of these materials were reviewed by Akiba and Okada [113].

2.2.3 Modified Binary Hydrides

MgH_2 is the binary hydride that has attracted by far the most attention as a potential storage material; however, there are two other binary hydrides that we should also mention, namely AlH_3 and PdH_x . The former is of interest due to its high gravimetric storage capacity of 10.1 wt% [114–116]. However, it is effectively non-reversible within a realistic hydrogen pressure range for a practical storage unit and therefore requires off-board regeneration. This process is economically and energetically costly, and non-reversible hydrides are beyond the scope of our discussion.¹² Palladium, meanwhile, is impractical as a storage material because of its relatively high operating temperature and low gravimetric capacity, as well as its high cost. However, research into nanoscale palladium [117–121] is being actively pursued due to the interesting differences seen in its hydrogen absorption behaviour compared to the bulk material. The hydrogen solubility of the hydride phase and equilibrium hydrogen pressures are reduced for small particles. The plateau region also slopes and narrows, and the critical temperature, T_{crit} , is significantly reduced in Pd clusters compared to the bulk

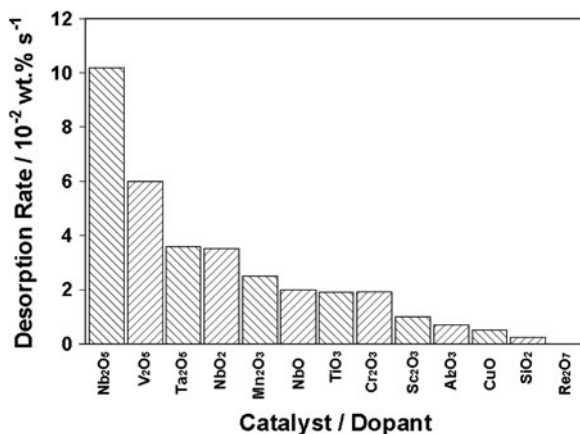
¹² AlH_3 is an example of a kinetically stabilised hydrogen storage material [114, 116], which are hydrides that have high equilibrium hydrogen pressures at ambient temperature but do not desorb appreciable amounts of hydrogen at this temperature due to kinetic limitations.

[120, 121]. Concomitantly, there is also a reduction in the enthalpies of hydride phase formation and decomposition. Similar effects are also seen for nanocrystalline samples [117]. From a practical point of view, the cost of Pd would seem to be prohibitive for widespread use, although it is possible that nanoscale Pd could find use as a catalyst in practical storage materials. Nevertheless, Pd hydride can be regarded as a model system for the investigation of size effects [118–120] and therefore continued study of this system is likely to provide further valuable insight into the effects of particle size reduction in other interstitial metal hydride systems.

Returning to magnesium, MgH_2 is an attractive potential storage material because it has a gravimetric capacity of 7.66 wt%. However, in addition to its high thermodynamic stability ($\Delta H \approx -75 \text{ kJ mol}^{-1} \text{ H}_2$), the kinetics of hydride formation and decomposition of the bulk material are too slow for practical purposes [122–124]. The kinetics have, however, been improved significantly using mechanical milling both with and without catalytic additives. The positive effects of ball-milling pure MgH_2 have been known since the late 1990s [123, 125], although the temperatures required for desorption are still too high for practical applications. The reviews of Huot et al. [123] and Zaluska et al. [125] both show the improvement in the kinetics at 573 K, for example. However, alternative methods of producing nanoscale magnesium have also been reported (see Gross et al. [126] and references therein), and include an electrochemical synthesis method reported recently by Aguey-Zinsou and Ares-Fernández [127], which results in an average particle size of approximately 5 nm.

With regard to the catalytic enhancement of the hydrogen absorption and desorption properties of MgH_2 , the most successful catalyst found to date appears to be Nb_2O_5 . The hydrogen desorption rates obtained using various oxide additives are shown in Fig. 2.3 [128]. The reasons for the enhanced absorption and desorption rates are not yet understood and it is possible that the additives do not act catalytically but instead induce further MgH_2 particle or grain size reduction during the milling process [129]. The results of a number of different additives,

Fig. 2.3 The catalytic effect of various transition metal oxides on the hydrogen desorption rate for MgH_2 [128]. Reaction rates were determined between 20 and 80% of the maximum hydrogen storage capacity in each case. Reprinted with permission from Barkhordian et al. [128]. Copyright 2006 American Chemical Society



including AB_5 and AB_2 intermetallics and elemental metals such as Ni and Ti, were tabulated by Sakintuna et al. [106]. In addition to the kinetic enhancement, there is some theoretical evidence that a reduced particle size can alter the thermodynamics of this system. Ab initio Hartree-Fock and density functional theory calculations, reported by Wagemans et al. [130], show that the stability of Mg hydride is reduced for very small cluster sizes below approximately 1.3 nm. Although this dimension is significantly smaller than the grain size achieved by mechanical milling, whether with or without an additive, these calculations demonstrate that there may be some potential for nanoscale magnesium hydride to provide hydrogen storage capabilities in a practical temperature range, although further work in this area is required. The use of magnesium hydride for hydrogen storage was recently reviewed by Grant [131].

2.2.4 Amorphous and Nanostructured Alloys

In this section we will look primarily at three types of amorphous and nanostructured alloy. Firstly, we will cover compounds that are synthesised or processed through the use of mechanical milling. This can have different effects on a material, depending on a number of factors. One possible effect is amorphisation, which is the loss of crystallographic order by an originally crystalline material. There are, however, a number of other ways to synthesise or process similarly amorphous alloys and so, secondly, we will discuss amorphous materials that can be produced using alternative routes. Thirdly, we will look at an interesting class of materials known as quasicrystals.

2.2.4.1 Mechanical Milling and Alloying

A significant area of research into new hydrogen storage materials involves the use of mechanical milling, as introduced in the section above for the modification of MgH_2 , for which it is well suited. The use of the technique originates from the development of Mechanical Alloying (MA), a powder processing method developed in the 1960s to produce oxide dispersion strengthened alloys [123, 132]. In materials processing there are a number of different types of milling with specific terminology used in each case [132]. For our purposes, the approaches applied to hydrogen storage material synthesis or modification can be broadly separated into three areas. Firstly, the synthesis of nanostructured or amorphous hydrogen-absorbing alloys using either elemental metals or the combination of elemental metals with crystalline intermetallics or alloys. Secondly, the nanostructuring or amorphisation of existing crystalline alloys or intermetallics through milling and, thirdly, the doping of an existing crystalline alloy or intermetallic with a catalytic additive. The latter is essentially the same as the approach used widely for magnesium hydride.

In each case mentioned above, the materials can benefit from the effects of the mechanical milling process, which includes the introduction of nanoscale structural features. Such nanostructuring can lead to size effects that are known to dramatically alter the behaviour of materials compared to bulk samples [133, 134] and the approach has a broad range of applications in materials science. Materials that have undergone milling can possess a smaller grain size, amorphous and disordered structural features, metastable and high pressure phases, an increased proportion of grain boundaries, a higher density of defects and an increased surface area [132]. All of these features can affect the hydrogen absorption properties of the material in comparison with unmilled, single phase, homogeneous crystalline samples [119, 120, 135]. If hydrogen diffusion occurs more rapidly through grain boundary regions, a smaller grain size will enhance the rate at which hydrogen is absorbed or desorbed. Also, amorphous phases of some compounds can show favourable absorption characteristics [136]. In addition, increased defect densities can enhance hydrogen diffusion rates. The activation process, which in many metallic absorbers involves the introduction of high dislocation densities into the host structure, can also be accelerated by milling the material. All of these factors can therefore potentially contribute to the improvement of the hydrogen storage properties of a material through milling. Although the process does not always have the desired effect, there is significant experimental evidence for the improvement of the hydrogen storage properties of materials through mechanical milling and alloying [123, 125, 137].

The different approaches mentioned above have been applied to a range of interstitial hydrides and hydride-forming hydrogen storage materials. Catalytic additives, such as Pd and Ni, have been milled with TiFe to improve the difficult activation process for this compound [138, 139]. Amorphous and crystalline hydrogen storage compounds that have been synthesised from the milling of elemental metals include $\text{Ni}_{1-x}\text{Zr}_x$ amorphous alloys [140], nanocrystalline LaNi_5 [141], amorphous and crystalline TiFe [142, 143], Ti–V–Mn alloys [144], and nanocrystalline Mg_2AlNi_2 [145], although many more examples can be found in the literature. The modification of crystalline alloys and intermetallics by milling, meanwhile, has included work on LaNi_5 [141, 146, 147], other AB_5 -based compounds [148, 149], Ti–Cr [150] and Ti–Cr–V [151, 152] alloys, and the Mg–Ni alloys [137, 153, 154] that can form complex transition metal hydrides (see Sect. 2.3.4). A further approach to the use of mechanical alloying is reactive milling in which the materials are processed in a hydrogen atmosphere [147, 151]. As intimated above, the milling process can also be damaging to the hydrogen sorption properties, as well as beneficial, with hydrogen absorption sometimes prevented entirely as a result of milling [144], or favourable isotherm behaviour being lost along with a significant amount of storage capacity [147, 150, 152]. However, increases in capacity as a result of milling have also been reported [149]. For interested readers, a recent monograph by Varin et al. [155] focuses primarily on the synthesis of hydrides for hydrogen storage through the use of mechanical milling.

2.2.4.2 Amorphous Alloys

In addition to the use of milling methods, amorphous alloys can also be produced using alternative synthesis routes. The methods include the rapid quenching of a melt, thermal evaporation, sputtering, electrodeposition and ion implantation [156, 157]. Many amorphous materials produced using these techniques can absorb significant amounts of hydrogen. Those of interest for hydrogen storage were summarised by Bowman [156] as being of the form $A_{1-y}B_y$, where A is an early transition metal or rare earth and B is a late transition metal, together with $Pd_{1-y}Si_y$. Examples of the former include $Ti_{1-y}Ni_y$, where $0.40 \leq y \leq 0.67$, $Zr_{1-y}Ni_y$, where $0.30 \leq y \leq 0.90$, $Zr_{1-y}Fe_y$, where y is 0.24 and 0.25, and $Y_{1-y}Fe_y$, where $0.25 \leq y \leq 0.55$. These compounds have maximum observed hydrogen-to-metal atom ratios (H/M) of 1.25, 1.4, 2.46 and 1.8, respectively. Unlike the crystalline intermetallic hydrides, these amorphous alloys tend to exhibit no plateau in their hydrogen absorption and desorption isotherms. This would seem to be a disadvantage in storage applications, in which the relatively large uptakes over small pressure changes in the plateau region are exploited (see Sect. 3.1.1). However, it has been argued that because this indicates the absence of hydride phase formation, the decrepitation that is associated with this process does not occur, which may lead to greater long term cycling stability. However, it is worth noting that the metastable state of these amorphous materials means that they can undergo recrystallisation if subjected to too high a temperature. For storage purposes, it would seem that these amorphous alloys would primarily be of interest if they absorb significantly more hydrogen than their crystalline counterparts, but this is only the case for some of these materials, such as $Ti_{1-y}Cu_yH_x$ and $Pd_{1-y}Si_yH_x$, although there appears to be some discrepancies in the literature. See the review of Eliaz and Eliezer [157] for further discussion of these points. Amorphous alloy systems are discussed in more detail by Fukai [81], with a focus on their thermodynamics, structure and the distributions of site energies in these materials, which differ significantly from ordered hydrides. It is worth noting that hydrogen absorption can itself induce amorphisation in some originally crystalline materials [81], although this phenomenon does not necessarily have an application in the field of hydrogen storage.

2.2.4.3 Quasicrystals

Quasicrystals are an interesting class of materials that show long range order but no translational symmetry. Since the first report in 1984 [158], over one hundred different quasicrystals have been synthesised [159, 160] and they have recently been reported to occur in nature [160]. Several quasicrystals have been investigated for their hydrogen storage properties, including alloys based on Ti–Zr–Ni [161, 162], Ti–Hf–Ni [162], and Mg–Al–Zn [163]. The promise of enhanced hydrogen storage capacities in these materials derives from the large number of

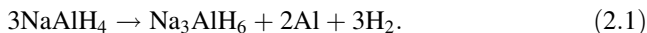
potential interstitial sites that exist in their structure. Takasaki and Kelton [162] found that a Ti-based quasicrystal of composition $\text{Ti}_{61}\text{Zr}_{22}\text{Ni}_{17}$ had a hydrogen storage capacity of 2.8 wt%, following electrochemical hydrogenation. The capacity of the $\text{Mg}_{44}\text{Al}_{15}\text{Zn}_{41}$ material studied by Bystrzycki et al. [163], meanwhile, was only 0.6 wt% at 100 bar (10.0 MPa) and temperatures of 573 and 673 K. Furthermore, the material was found to decompose into a MgZn_2 phase and MgH_2 following hydrogenation. Although this latter result does not seem particularly promising, further work is undoubtedly necessary to determine whether other quasicrystalline compounds could serve as effective hydrogen storage materials.

2.3 Complex Hydrides

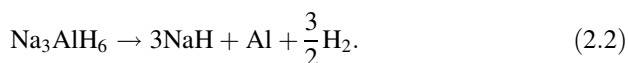
In the case of complex hydrides, atomic hydrogen is bound either ionically or covalently into the bulk of the storage material. It is then released via the decomposition of the host into two or more components. These materials are generally formed from alkali or alkaline earth metals and $[\text{AlH}_4]^-$, $[\text{NH}_2]^-$ and $[\text{BH}_4]^-$ anionic hydrides. As with many of the materials covered in this chapter, complex hydrides were first synthesised many years ago but it is only through recent work that their potential use as practical reversible hydrogen storage materials has been realised. This has occurred, most notably, in the case of sodium alanate (NaAlH_4), due to the discovery of the catalytic enhancement by Ti-doping of the hydrogenation/dehydrogenation process by Bogdanović and Schwickardi [164], but also by the discovery of the reversible hydrogen sorption properties of the Li–N–H system by Chen et al. [165]. The term *complex hydride* has become an umbrella term encompassing the alanates, nitrides and borohydrides that are currently being considered for hydrogen storage [166, 167]. In this section, we cover each of these in turn and also look at the A_2BH_x compounds that are classed as complex transition metal hydrides.

2.3.1 Alanates

The prototype hydrogen storage material in this group is sodium alanate, NaAlH_4 . Its structure consists of sodium atoms surrounded by $[\text{AlH}_4]^-$ tetrahedra. During the dehydrogenation process this phase decomposes into an intermediate Na_3AlH_6 phase with an associated release of gaseous hydrogen,



A second reaction step then results in further hydrogen evolution,



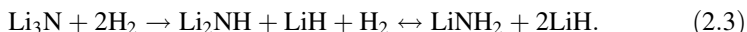
Reaction (2.1) occurs between approximately 210 and 220°C (483 and 493 K), and reaction (2.2) around 250°C (523 K). The dehydrogenation of NaH does not occur until approximately 425°C (698 K) and does not, therefore, play a practical role in the reversible hydrogen storage process. The two stage reaction results in an isotherm with two plateaus. At 210°C (483 K), plateau pressures of 15.4 and 2.1 MPa were determined by Dymova et al. [168]. The irreversibility of this reaction, the instability of the hydride and the slow desorption kinetics meant that this material was not considered a particularly promising storage material. The breakthrough came in the mid 1990s when Bogdanović and Schwickardi [164] discovered the remarkable effect that the addition of TiCl_3 has on the reversibility and the kinetics of the hydrogenation process. Jensen et al. [169, 170] subsequently improved on Bogdanović and Schwickardi's wet chemistry doping method and showed that further improvements could be made through mechanical mixing of the alanate and the dopant compounds. Since this early work, many other effective dopants have been identified, including ScCl_3 , CeCl_3 and PrCl_3 [168, 171].

Ti-doped NaAlH_4 readily desorbs hydrogen at temperatures in the region of 120°C (393 K) and can be rehydrogenated at 170°C (443 K) in 15 MPa of hydrogen [172]. Although the role of the Ti catalyst is not yet fully understood [173], this material has already been used in practical hydrogen storage units, and so it has proved to a certain extent that complex hydrides can be practically applied to storage applications. Applied research into the use of sodium alanate is now at a reasonably advanced stage; a recent study, for example, investigated the safety of a sodium alanate store by experimentally simulating a tank failure and the subsequent expulsion of sodium alanate powder [174]. The expelled dust cloud did not spontaneously ignite, but the presence of an external ignition source resulted in a flame of reacting powder. Ignition also occurred when water was sprayed onto the expelled dust cloud. This result is relatively positive because spontaneous ignition may be expected but was not observed.

Other alanates that are being considered for hydrogen storage include LiAlH_4 , KAlH_4 , $\text{Mg}(\text{AlH}_4)_2$ and $\text{Ca}(\text{AlH}_4)_2$, which have gravimetric hydrogen capacities of 10.54, 5.71, 9.27 and 7.84 wt%, respectively. A number of mixed alanates have also been reported in the literature, including $\text{Na}_2\text{LiAlH}_6$, K_2NaAlH_6 , K_2LiAlH_6 and $\text{LiMg}(\text{AlH}_4)_3$ [115, 175] and recent work has investigated various mixed alanate combinations, including Mg–Li–Al–H [176], Mg–Ca–Al–H, Li–Ca–Al–H and Na–Ca–Al–H [177], and Mg–Na–Al–H, Mg–K–Al–H and Ca–K–Al–H [178], although work on these systems is still at an early stage. Continued research in the area will hopefully reveal new alanates, new alanate phases or mixed alanate combinations, as well as new catalysts, particularly if significant progress can be made in understanding the role of the Ti dopant. Hydrogen storage using NaAlH_4 , LiAlH_4 , KAlH_4 and $\text{Mg}(\text{AlH}_4)_2$ was reviewed by Jensen et al. [168], with a focus on Ti-doped sodium alanate.

2.3.2 Nitrides, Amides and Imides

The potential of the Li–N–H system as a potential storage material was first reported by Chen et al. [165]. The system forms three stoichiometric ternary compounds: *lithium imide* (Li_2NH), *lithium amide* (LiNH_2) and *lithium nitride hydride* (Li_4NH). The latter, however, is not involved in the proposed reversible hydrogen storage process. This begins with lithium nitride (Li_3N), which is hydrogenated to form a combination of lithium imide and lithium hydride (LiH). Further hydrogenation results in the formation of lithium amide and further lithium hydride, and the complete process is represented by the following reaction,



Dehydrogenation of the imide requires high vacuum and temperatures above 600 K [165]. These are unsuitable conditions for reversible hydrogen storage, but the reaction between the imide and the amide is reversible under more moderate conditions of both temperature and pressure. The mixed hydride/imide on the right-hand side of reaction (2.3) gives a high theoretical hydrogen capacity of 10.4 wt%, but the reversible capacity between the imide and amide is approximately 6.5 wt% (one H_2 molecule released from $\text{LiNH}_2 + 2\text{LiH}$).¹³

A number of other similar materials have been studied as hydrogen storage media, including the ternary compounds $\text{Mg}(\text{NH}_2)_2$, RbNH_2 , CsNH_2 and Ca–N–H , and the quarternary and higher systems Li–Ca–N–H , Li–Al–N–H , Na–Mg–N–H , Na–Ca–N–H , Mg–Ca–N–H and Li–Mg–Ca–N–H [167]. It can be seen that these materials have the potential to provide high gravimetric storage capacities and are therefore of great interest. However, the Li–N–H system suffers from a number of drawbacks, including the high hydrogenation and dehydrogenation temperatures, and air or moisture sensitivity. Another is the evolution of ammonia during the dehydrogenation reaction [180]. As well as contributing to the degradation of samples during long term cycling, the evolution of ammonia is also an issue because it is a very effective poison for PEM fuel cell membranes [181]. The storage of hydrogen using imides and amides, including mixed systems, was reviewed recently by Gregory [182].

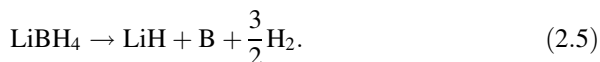
2.3.3 Borohydrides

Borohydrides have the highest gravimetric hydrogen storage capacities of any of the complex hydrides. LiBH_4 contains 18.5 wt% hydrogen, and releases it through one of the following two reactions [183],

¹³ A theoretical capacity of 11.5 wt% is occasionally quoted but this value, depending on the definition of hydrogen capacity, is an error from the original Chen et al. [165] paper that has since appeared in other reports [179].



or,



However, the decomposition temperature is too high for practical purposes. According to Orimo et al. [167], LiBH_4 releases three of its four hydrogen atoms upon melting at 280°C (553 K), with an enthalpy of decomposition of $-88.7 \text{ kJ mol}^{-1} \text{ H}_2$. LiH is very stable and its dehydrogenation occurs only above a temperature of 727°C (1000 K). Nevertheless, the dehydrogenation reaction of LiBH_4 is a reversible process, although rehydrogenation requires elevated pressures and temperatures of 35.0 MPa at 600°C (873 K) and 20.0 MPa at 690°C (963 K). As for most of the complex hydrides, the hydrogenation mechanism of LiH and B is not yet understood, but it is thought to result either from the intermediate reaction of LiH with B , to form a compound that is subsequently filled with hydrogen, or from the reaction of B and H to form diborane, which then spontaneously reacts with LiH to give the full borohydride [167].

A number of other alkali metal and alkaline earth metal borohydrides have high gravimetric and volumetric hydrogen storage capacities. For example, the theoretical gravimetric capacities of NaBH_4 , KBH_4 , and $\text{Mg}(\text{BH}_4)_2$ are 10.6, 7.4 and 14.8 wt%, with volumetric capacities of 113.1, 87.1 and 146.5 kg m^{-3} , respectively. However, these are all theoretical values and cannot be reversibly achieved in practice at practical temperatures; borohydrides are also moisture sensitive [184] and Eberle et al. [173] suggest that the possible evolution of volatile boranes, even at trace levels, would be problematic due to storage capacity loss and fuel cell damage. However, as for all of the complex hydrides, their high theoretical capacities mean that further work on these materials would be valuable. Nakamori and Orimo [184] recently reviewed hydrogen storage using borohydrides, including those suitable for both reversible and non-reversible chemical hydrogen storage. Walker [185], meanwhile, discussed the destabilisation of complex hydrides via mixing with other compounds, focusing on the use of this strategy for LiBH_4 with various additives including hydrides (MgH_2), magnesium salts (MgF_2 , MgS_2 and MgSe_2), elemental metals (Al), alloys, oxides (TiO_2) and carbon. This offers an interesting route for the modification of borohydrides, as well as other complex hydrides, for hydrogen storage applications, and is likely to be the subject of continued research.

2.3.4 Complex Transition Metal Hydrides

A number of complex transition metal hydrides have been known for some time to reversibly desorb and absorb hydrogen. Examples of these materials include Mg_2FeH_6 , Mg_2NiH_4 and Mg_2CoH_5 [95]. Some of the host metallic constituents form stable intermetallics, such as Mg_2Ni and Mg_2Cu , but most do not. The complex transition metal hydrides include compounds with impressive storage

capabilities, including a H/M ratio of 4.5 in the case of BaReH_9 and a volumetric capacity of approximately 150 g L^{-1} , twice that of liquid hydrogen, as is the case for Mg_2FeH_6 [95].

Mg_2NiH_4 is the material in this group that has probably received the most attention as a candidate storage material, due in part to its gravimetric hydrogen capacity of 3.6 wt%. Its synthesis was first reported by Reilly and Wiswall [90] and it was long considered to be an interstitial hydride, but its structure is now known to consist of tetrahedral NiH_4 complexes [186–188]. Complex transition metal hydrides generally suffer from the same problem as the other complex hydrides currently being considered for hydrogen storage, namely the high absorption and desorption temperatures. Mg_2NiH_4 has an enthalpy of formation of $-32.3 \text{ kJ mol}^{-1}$ H and requires temperatures above 520 K for hydrogen desorption, and higher temperatures still for absorption. Progress has, however, been made on the destabilisation of this material through mechanical milling (Sect. 2.2.4) [186]. A decrease of the hydrogen desorption temperature in mechanically milled Mg_2Ni was attributed by Orimo and Fujii [137, 186] to the presence of a large proportion of grain boundaries following the milling process. However, the hydrogen storage capacity was concomitantly decreased to 1.6 wt% in the milled material.

Although these materials have not recently received as much attention as the alanates, amides and imides, and borohydrides, they are prominent examples of another type of non-interstitial hydride. It seems likely that there are many more, as yet undiscovered, multinary complex hydride compounds that could potentially serve as effective hydrogen storage materials. Therefore, although they do not necessarily exhibit gravimetric capacities in excess of the US DOE targets, continued work into new complex hydride compounds, such as the complex transition metal hydrides, may yet prove fruitful.

2.4 Other Materials

In the last three sections we have covered a range of potential reversible storage materials grouped into the porous adsorbents, interstitial hydrides and complex hydrides. In this section we look at materials that do not fit readily into these categories, which include the clathrates and ionic liquids. We shall also look at materials that show enhanced hydrogen storage through the mechanism of hydrogen spillover. Although the latter are principally porous adsorbents, the proposed storage mechanism is fundamentally different to molecular physisorption, as covered in Sect. 2.1; hence its separate treatment.

2.4.1 Clathrates

Clathrate hydrates are a novel proposed solution to the hydrogen storage problem. They are inclusion compounds formed from hydrogen-bonded networks of water

molecules and have long been known due to their occurrence in natural gas and oil pipelines [189]. The guests can include species such as methane, nitrogen and argon, but the discovery of molecular hydrogen encapsulation by Mao et al. [190] has led to the study of clathrates for solid state hydrogen storage [191]. Although pure hydrogen clathrate hydrates are stable only at high pressures or low temperatures, recent work has shown that they can be stabilised under near-ambient conditions using a promoter such as Tetrahydrofuran (THF) [191, 192]. There are three clathrate hydrate structures, namely sI, sII and sH, and the latter two have been studied for their hydrogen storage properties.

Some controversy has surrounded the capacity of sII after an initial report by Lee et al. [193] of a potential hydrogen storage capacity of 4 wt% and the ability to tune the clathrates by varying the THF concentration. These results have not been independently verified, and it seems that the consensus is a practical maximum storage capacity closer to 1 wt% [194]. Recently, hydrogen storage in the sH phase has been proposed, with estimated capacities in the region of 1.4 wt% [195–197]. The stabilisation of sH has been achieved using alternative promoters, including Methyl *tert*-Butyl Ether (MTBE) and 1,1-Dimethylcyclohexane (DMCH) [196, 197]. The reduced capacities of the stabilised clathrates, and hence the source of some of the controversy, originates from the occupancy of a proportion of the cages in the clathrate structures by the promoter molecules rather than hydrogen. In the case of sII, it was argued that reducing the quantity of THF used to stabilise the clathrate allowed hydrogen to occupy some of the larger cages occupied by THF at higher concentrations, thus allowing significantly higher hydrogen storage capacities to be achieved [193]. However, the occupation of these larger cavities by hydrogen was subsequently disputed by other authors [194]. In addition to hydrogen storage in clathrate hydrates, the possibility of hydrogen storage in the organic clathrate hydroquinone (1,4-benzenediol) has also been reported recently [198–200]. As for many of the materials covered in this chapter, hydrogen storage using both clathrate hydrates and alternative organic clathrates is the subject of ongoing research.

One significant disadvantage of clathrates is the slow rate of clathrate formation. In recent work, Cooper et al. have demonstrated that clathrates stabilised in the pores of emulsion templated polymers¹⁴ [201] and formed in hydrophilic water-swelling polymer network¹⁵-based hydrogels [202] show potential for hydrogen storage applications. Although the reported capacities are low, such supported clathrate formation appears to greatly enhance the kinetics of the process and is therefore an interesting area for further research.

¹⁴ Ultralow density, emulsion-templated polymerized High Internal Phase Emulsion (polyHIPE) material.

¹⁵ Lightly crosslinked poly(acrylic acid) sodium salt (PSA).

2.4.2 Ionic Liquids

Ionic liquids have been attracting significant amounts of attention due to their use in catalysis, as so-called green solvents and in a vast array of other applications [203, 204]. They are defined as materials composed of cations and anions which melt at or below 100°C (373 K) [203], and their negligible vapour pressures mean that they are environmentally-friendly in comparison to the volatile organic solvents that they can potentially replace in many industrial and chemical processes. Stracke et al. [205] recently reported the potential of imidazolium ionic liquids for hydrogen storage, with a volumetric hydrogen capacity of up to 30 g L⁻¹. However, the dehydrogenation temperature of the Pd/C-catalysed material¹⁶ was in the region 230 to 300°C (503 to 573 K) and the hydrogenation time was approximately 100 hours. Although this performance does not appear particularly encouraging, it is worth bearing in mind that, according to Plechkova and Seddon [203], there are over one million simple ionic liquids, and many more binary and ternary systems. Therefore, further work is certainly required if a meaningful conclusion on the suitability of this interesting class of materials for hydrogen storage applications is to be drawn.

2.4.3 The Use of Hydrogen Spillover

Extensive research on the exploitation of spillover for hydrogen storage has been carried out in recent years [206, 207]. *Spillover* is a mechanism by which molecular hydrogen dissociates on catalytically active particles and subsequently migrates to the surface of a solid state support that would not otherwise adsorb or absorb the atomic hydrogen under the same conditions [208]. For this to occur, a porous material must be doped with suitably catalytic nanoparticles to facilitate the dissociation process. It is a well documented, yet poorly understood, phenomenon in heterogeneous catalysis [208] and has been proposed as a way of enhancing the storage capacity of porous materials at near-ambient temperature. The proposed methods for producing high capacity storage materials include physical mixing of a supported catalyst with a secondary (receptor) material, the use of carbon bridges between a supported catalyst and the receptor, and the direct doping of the receptor with the catalyst [206]. The first two of these use so-called *secondary spillover*. In the case of the carbon bridge-building approach, the carbon bridges are formed from a carbon precursor, such as glucose, which is subsequently carbonised by heating. This forms a carbon bridge between the supported catalyst, such as Pd on carbon, and a secondary receptor, such as an activated carbon. At 298 K, this method was found to enhance the storage capacity of an activated carbon (AX-21) by a factor of 2.9 [209]. The carbon bridge-building approach has also been

¹⁶ 1-alkyl(aryl)-3-methylimidazolium *N*-bis(trifluoromethanesulfonyl) salt.

applied to MOFs using a carbon precursor that does not require carbonisation temperatures high enough to decompose the metal-organic framework support, although simple physical mixing of a supported catalyst has also been used. The doping of various metallic catalysts, such as Ni, Pd, Pt and Ru, has been performed via chemical, ultrasonic and plasma-assisted methods on a range of carbon supports [206]. The capacities claimed for room temperature hydrogen storage using the spillover mechanism show improvement over undoped materials; however, it remains to be seen whether significant enhancement in the reversible storage density of hydrogen can be achieved using this approach.

2.4.4 Organic and Inorganic Nanotubes

We will close this section by mentioning some nanostructured materials closely related to the carbon nanotubes covered in [Sect. 2.1.1.2](#). As we saw in that section, carbon nanotubes have received a great deal of attention as potential storage materials, but many other *organic* and *inorganic nanotube materials* also exist. The review by Rao and Nath [210] provides a good overview of inorganic nanotubes and their synthesis, including chalcogenide, oxide and nitride nanotube materials. A number of these, in particular those consisting of lighter elements, have been investigated for their hydrogen storage properties. Three types were covered by Seayad and Antonelli [211]: boron nitride (BN) [212, 213], titanium sulfide (TiS_2) [214] and molybdenum sulfide (MoS_2) nanotubes [215], with reported capacities reaching 4.2 wt% for collapsed BN nanotubes at 10 MPa and ambient temperature [216]. In addition, other materials in nanotube form have since been investigated either experimentally or theoretically for their hydrogen storage properties, including titanium oxide (TiO_2) [211, 217], tungsten carbide (WC) [218], silicon [219] and silicon carbide (SC) [220], and the hydrogen sorption properties of some of these materials appear very interesting. For example, the ability of some multiwalled nanotubes to intercalate other species [210, 211] provides a possible proposed mechanism that could allow significant amounts of hydrogen to be stored at practical temperatures [217]. However, the suitability of these nanostructured materials for a large scale application, such as automotive transportation, remains open to question.

2.5 Summary

In this chapter we have presented an overview of the various types of materials that are currently being considered as potential reversible hydrogen storage media. We began with microporous materials, which include carbons, zeolites, metal-organic frameworks and microporous organic polymers, before moving on to the interstitial hydrides. Microporous materials store molecular hydrogen adsorbed in

Table 2.1 A comparison of the basic hydrogen storage properties of a number of reversible hydrogen storage material types, and other physical and chemical storage methods. Note that absolute comparisons between the values given in this table, and others published widely elsewhere, are difficult because of the use of different definitions of storage capacity, particularly between different storage material types, and the significant effect of the hydrogen pressure and the temperature on quoted capacity values. In addition, isotherm shape can greatly affect the reversible capacity in comparison with the total capacity. As a result, these values should be treated only as an approximate guide and care should be exercised in attempts to draw a firm conclusion from direct comparisons. Further discussion of the different capacity definitions and other related considerations are given in the following chapter

Category / storage method	Material / storage medium	Gravimetric capacity ^a (wt%) (P/MPa)	Volumetric capacity ^a (g L ⁻¹ or kg m ⁻³)	Operating temperature region	References
Pure H ₂	Compressed (70 MPa)	100(70)	39.0 ^b	ambient	[44]
	Liquid	4.8, with tank 100	23.0, with tank 70.8	20 K	[221]
Chemical hydrides (hydrocarbons)	Cyclohexane (C ₆ H ₁₂)	7.2 ^c	28.0	508–623 K ^d	[221]
	<i>cis</i> -decalin	7.3 ^e	32.7	483 K ^f	[221]
	<i>trans</i> -decalin	7.3 ^e	31.7	483 K ^f	[221]
Chemical hydrides (other)	NaBH ₄	10.57	113.1	778 K	[167]
	Mg(NH ₃) ₆ Cl ₂	9.2	110	> 400 K	[222]
Binary hydrides	AlH ₃	10.1	148	< 373 K	[116]
Microporous adsorbents	Zeolite-templated carbon	6.9(2.0)	–	77 K	[26]
	Na-X zeolite	2.55(4.0)	–	77 K	[35]
	MOF-5	5.25(4.85)	31.0	77 K	[56]
	MOF-177	7.52(6.85)	32.1	77 K	[56]
	trip-PIM	2.7(1.0)	–	77 K	[66]
	HCP (BCMBP-based)	3.68(1.5)	–	77 K	[68]
	COF-102	7.24(4.0)	29 (excess) ^g 48 (absolute) ^g	77 K	[70]
	EOF-2	1.21(0.1)	–	77 K	[76]

(continued)

Table 2.1 (continued)

Category / storage method	Material / storage medium	Gravimetric capacity ^a (wt%) (P/MPa)	Volumetric capacity ^a (g L ⁻¹ or kg m ⁻³)	Operating temperature region	References
Interstitial hydrides	TiFe	1.86/1.5	100.4/83.7	near ambient	[87, 223]
	Ti _{0.98} Zr _{0.02} Cr _{0.05} V _{0.43} Fe _{0.09} Mn _{1.5}	1.9/1.3	63.6	near ambient	[87]
	LaNi ₅	1.49/1.28	87.0	near ambient	[87]
	LaNi _{4.8} Sn _{0.2}	1.4/1.24	85.4	near ambient	[87]
	(V _{0.9} Ti _{0.1}) _{0.95} Fe _{0.05}	1.95/1.8	82.0	near ambient	[87]
Complex hydrides	Nb ₂ O ₅ -doped MgH ₂	≈ 7	112.1 ^h	≈ 573 K	[128, 223]
	NaAlH ₄	7.47/5.6	–	373–473 K	[167]
	LiNH ₂ + 2LiH	10.4/6.5	–	≈ 573 K	[224]
	LiBH ₄	18.36/5–10 ⁱ / 13.5 ^j	122.5	453–923 K	[167]
	Mg ₂ NiH ₄	3.6/3.3	98.8/87.0	> 528 K	[87, 223]
Clathrates	THF-stabilised H ₂ clathrate	≈ 1	–	270–280 K	[191]
RTILs	Imidazolium RTIL	–	30	503–573 K	[205]
Nanotubes	“Collapsed” BN	4.2(10.0)	–	ambient	[216]
	TiO ₂	≈ 4(0.6)	–	77 K	[217]

^a Reversible capacity shown in *italics*, where appropriate
^b Density at 70.0 MPa and 300 K calculated using NIST REFPROP database [225]
^c Hydrogen released during dehydrogenation to benzene
^d Temperature required for dehydrogenation [221]
^e Hydrogen released during dehydrogenation to naphthalene
^f Temperature required for dehydrogenation [226]
^g Estimated from adsorption isotherm at approximately 8.5 MPa
^h Calculated from the value for MgH₂ given by Wiswall [223]
ⁱ Observed rehydrogenation
^j Observed first dehydrogenation

their pores at relatively low temperatures and, in certain cases, can achieve gravimetric storage capacities on a materials basis in excess of the current 2015 US DOE system storage target. The interstitial hydrides absorb atomic hydrogen into the bulk of a metallic host material and, although they do not possess particularly high gravimetric capacities, they exhibit impressive volumetric hydrogen storage capabilities and some favourable hydrogen storage properties. The third type of storage material we have considered are the complex hydrides. This group of compounds, like the interstitial hydrides, store atomic hydrogen in their bulk but, in this case, bond the hydrogen in complexes. Upon hydrogen desorption, their host structure decomposes to one or more additional decomposition products. We concluded the chapter by considering some materials that do not fit readily into the other three main categories, including clathrates, ionic liquids and inorganic nanotubes. Some of the basic hydrogen storage properties of materials covered in this chapter are summarised in Table 2.1.

References

1. Sing KSW, Everett DH, Haul RAW, Moscou L, Pierotti RA, Rouquérol J, Siemienińska T (1985) Reporting physisorption data for gas/solid systems with special reference to the determination of surface area and porosity. *Pure Appl Chem* 57(4):603–619
2. Menon VC, Komarneni S (1998) Porous adsorbents for vehicular natural gas storage: a review. *J Porous Mater* 5:43–58
3. McBain JW (1909) The mechanism of the adsorption (“sorption”) of hydrogen by carbon. *Philos Mag Ser 6* 18(108):916–935
4. Frolich PK, White A (1930) Adsorption of methane and hydrogen on charcoal at high pressure. *Ind Eng Chem* 22(10):1058–1060
5. Carpetis C, Peschka W (1980) A study on hydrogen storage by use of cryoadsorbents. *Int J Hydrogen Energy* 5:539–554
6. Agarwal RK, Noh JS, Schwarz JA, Davini P (1987) Effect of surface acidity of activated carbon on hydrogen storage. *Carbon* 25(2):219–226
7. Chahine R, Bose TK (1994) Low-pressure adsorption storage of hydrogen. *Int J Hydrogen Energy* 19(2):161–164
8. Férey G (2008) Hybrid porous solids: past, present, future. *Chem Soc Rev* 37:191–214
9. Rouquerol F, Rouquerol J, Sing K (1999) Adsorption by powders and porous solids: principles, methodology and applications. Academic Press, London
10. Menon PG (1968) Adsorption at high pressures. *Chem Rev* 68(3):277–294
11. Broom DP, Walton A, Book D, Benham MJ (2007) The accurate determination of the temperature dependence of hydrogen uptake by Na-X zeolite. Presented at the 15th International Zeolite Conference, Beijing, China, 12–17 August 2007
12. Thomas KM (2009) Adsorption and desorption of hydrogen on metal-organic framework materials for storage applications: comparison with other nanoporous materials. *Dalton Trans* 1487–1505
13. Yürüm Y, Taralp A, Veziroglu TN (2009) Storage of hydrogen in nanostructured carbon materials. *Int J Hydrogen Energy* 34:3784–3798
14. Rzepka M, Lamp P, de la Casa-Lillo MA (1998) Physisorption of hydrogen on microporous carbon and carbon nanotubes. *J Phys Chem B* 102:10894–10898
15. Jordá-Beneyto M, Suárez-García F, Lozano-Castelló D, Cazorla-Amorós D, Linares-Solano A (2007) Hydrogen storage on chemically activated carbons and carbon nanomaterials at high pressures. *Carbon* 45:293–303

16. Zlotea C, Moretto P, Steriotis T (2009) A Round Robin characterisation of the hydrogen sorption properties of a carbon based material. *Int J Hydrogen Energy* 34(7):3044–3057
17. Jordá-Beneyto M, Lozano-Castelló D, Suárez-García F, Cazorla-Amorós D, Linares-Solano Á (2008) Advanced activated carbon monoliths and activated carbons for hydrogen storage. *Microporous Mesoporous Mater* 112:235–242
18. Dillon AC, Jones KM, Bekkedahl TA, Kiang CH, Bethune DS, Heben MJ (1997) Storage of hydrogen in single-walled carbon nanotubes. *Nature* 386:377–379
19. Züttel A, Orimo S (2002) Hydrogen in nanostructured, carbon-related, and metallic materials. *MRS Bull* 27(9):705–711
20. Hirscher M, Becher M, Haluska M, Dettlaff-Weglikowska U, Quintel A, Duesberg GS, Choi Y-M, Downes P, Hulman M, Roth S, Stepanek I, Bernier P (2001) Hydrogen storage in sonicated carbon materials. *Appl Phys A* 72:129–132
21. Chambers A, Park C, Baker RTK, Rodriguez NM (1998) Hydrogen storage in graphite nanofibers. *J Phys Chem B* 102(22):4253–4256
22. Lamari Darkrim F, Malbrunot P, Tartaglia GP (2002) Review of hydrogen storage by adsorption in carbon nanotubes. *Int J Hydrogen Energy* 27:193–202
23. Blackman JM, Patrick JW, Snape CE (2006) An accurate volumetric differential pressure method for the determination of hydrogen storage capacity at high pressures in carbon materials. *Carbon* 44:918–927
24. Pubysheva OV, Farajian AA, Yakobson BI (2008) Fullerene nanocage capacity for hydrogen storage. *Nano Lett* 8(3):767–774
25. Xu W-C, Takahashi K, Matsuo Y, Hattori Y, Kumagai M, Ishiyama S, Kaneko K, Iijima S (2007) Investigation of hydrogen storage capacity of various carbon materials. *Int J Hydrogen Energy* 32:2504–2512
26. Yang Z, Xia Y, Mokaya R (2007) Enhanced hydrogen storage capacity of high surface area zeolite-like carbon materials. *J Am Chem Soc* 129:1673–1679
27. Hu Q, Lu Y, Meisner GP (2008) Preparation of nanoporous carbon particles and their cryogenic hydrogen storage capacities. *J Phys Chem C* 112:1516–1523
28. Gogotsi Y, Dash RK, Yushin G, Yildirim T, Laudisio G, Fischer JE (2005) Tailoring of nanoscale porosity in carbide-derived carbons for hydrogen storage. *J Am Chem Soc* 127:16006–16007
29. Gogotsi Y, Portet C, Osswald S, Simmons JM, Yildirim T, Laudisio G, Fischer JE (2009) Importance of pore size in high-pressure hydrogen storage by porous carbons. *Int J Hydrogen Energy* 34:6314–6319
30. Baerlocher Ch, Yoshikawa T, McCusker LB, Olson DH (2007) *Atlas of zeolite framework types*, 6th edn. Elsevier, Amsterdam
31. Nijkamp MG, Raaymakers JEMJ, van Dillen AJ, de Jong KP (2001) Hydrogen storage using physisorption - materials demands. *Appl Phys A* 72:619–623
32. Vitillo JG, Ricchiardi G, Spoto G, Zecchina A (2005) Theoretical maximal storage of hydrogen in zeolitic frameworks. *Phys Chem Chem Phys* 7:3948–3954
33. Langmi HW, Walton A, Al-Mamouri MM, Johnson SR, Book D, Speight JD, Edwards PP, Gameson I, Anderson PA, Harris IR (2003) Hydrogen adsorption in zeolites A, X, Y and RHO. *J Alloy Compd* 356–357:710–715
34. Anderson PA (2008) Storage of hydrogen in zeolites. In: Walker G (ed) *Solid-state hydrogen storage: materials and chemistry*. Woodhead Publishing, Cambridge
35. Du X, Wu E (2006) Physisorption of hydrogen in A, X and ZSM-5 types of zeolites at moderately high pressures. *Chin J Chem Phys* 19(5):457–462
36. van den Berg AWC, Bromley ST, Jansen JC (2005) Thermodynamic limits on hydrogen storage in sodalite framework materials: a molecular mechanics investigation. *Microporous Mesoporous Mater* 78:63–71
37. van den Berg AWC, Bromley ST, Wojdel JC, Jansen JC (2006) Adsorption isotherms of H₂ in microporous materials with SOD structure: a grand canonical Monte Carlo study. *Microporous Mesoporous Mater* 87:235–242

38. Song MK, No KT (2007) Molecular simulation of hydrogen adsorption in organic zeolite. *Catal Today* 120:374–382
39. Fraenkel D, Shabtai J (1977) Encapsulation of hydrogen in molecular sieve zeolites. *J Am Chem Soc* 99:7074–7076
40. Efstathiou AM, Suib SL, Bennett CO (1990) Encapsulation of molecular hydrogen in zeolites at 1 atm. *J Catal* 123:456–462
41. Weitkamp J, Fritz M, Ernst S (1995) Zeolites as media for hydrogen storage. *Int J Hydrogen Energy* 20(12):967–970
42. Garrone E, Bonelli B, Otero Areán C (2008) Enthalpy-entropy correlation for hydrogen adsorption on zeolites. *Chem Phys Lett* 456:68–70
43. Otero Areán C, Turnes Palomino G, Llop Carayol MR (2007) Variable temperature FT-IR studies on hydrogen adsorption on the zeolite (Mg, Na)-Y. *Appl Surf Sci* 253:5701–5704
44. Felderhoff M, Weidenthaler C, von Helmolt R, Eberle U (2007) Hydrogen storage: the remaining scientific and technological challenges. *Phys Chem Chem Phys* 9:2643–2653
45. van den Berg AWC, Otero Areán C (2008) Materials for hydrogen storage: current research trends and perspectives. *Chem Commun* 668–681
46. Rosseinsky MJ (2004) Recent developments in metal-organic framework chemistry: design, discovery, permanent porosity and flexibility. *Microporous Mesoporous Mater* 73:15–30
47. Rowsell JLC, Yaghi OM (2004) Metal-organic frameworks: a new class of porous materials. *Microporous Mesoporous Mater* 73:3–14
48. Rowsell JLC, Yaghi OM (2005) Strategies for hydrogen storage in metal-organic frameworks. *Angew Chem Int Ed* 44:4670–4679
49. Collins DJ, Zhou HC (2007) Hydrogen storage in metal-organic frameworks. *J Mater Chem* 17:3154–3160
50. Zhao D, Yuan D, Zhou H-C (2008) The current status of hydrogen storage in metal-organic frameworks. *Energy Environ Sci* 1:222–235
51. Dincă M, Long JR (2008) Hydrogen storage in microporous metal-organic frameworks with exposed metal sites. *Angew Chem Int Ed* 47(36):6766–6779
52. Murray LJ, Dincă M, Long JR (2009) Hydrogen storage in metal-organic frameworks. *Chem Soc Rev* 38:1294–1314
53. Rosi NL, Eckert J, Eddaoudi M, Vodak DT, Kim J, O’Keefe M, Yaghi OM (2003) Hydrogen storage in microporous metal-organic frameworks. *Science* 300:1127–1129
54. Züttel A (2003) Materials for hydrogen storage. *Mater Today* 6(9):24–33
55. Rowsell JLC, Millward AR, Park KS, Yaghi OM (2004) Hydrogen sorption in functionalized metal-organic frameworks. *J Am Chem Soc* 126:5666–5667
56. Wong-Foy AG, Matzger AJ, Yaghi OM (2006) Exceptional H₂ saturation uptake in microporous metal-organic frameworks. *J Am Chem Soc* 128:3494–3495
57. Dincă M, Dailly A, Liu Y, Brown CM, Neumann DA, Long JR (2006) Hydrogen storage in a microporous metal-organic framework with exposed Mn²⁺ coordination sites. *J Am Chem Soc* 128:16876–16883
58. Kubas GJ (2007) Fundamentals of H₂ binding and reactivity on transition metals underlying hydrogenase function and H₂ production and storage. *Chem Rev* 107:4152–4205
59. Hoang TKA, Antonelli DM (2009) Exploiting the Kubas interaction in the design of hydrogen storage materials. *Adv Mater* 21:1787–1800
60. Zhao X, Xiao B, Fletcher AJ, Thomas KM, Bradshaw D, Rosseinsky MJ (2004) Hysteretic adsorption and desorption of hydrogen by nanoporous metal-organic frameworks. *Science* 306:1012–1015
61. Fletcher AJ, Thomas KM, Rosseinsky MJ (2005) Flexibility in metal-organic framework materials: impact on sorption properties. *J Solid State Chem* 178(8):2491–2510
62. Panella B, Hirscher M, Pütter H, Müller U (2006) Hydrogen adsorption in metal-organic frameworks: Cu-MOFs and Zn-MOFs compared. *Adv Funct Mater* 16:520–524
63. Chen B, Zhao X, Putkham A, Hong K, Lobkovsky EB, Hurtado EJ, Fletcher AJ, Thomas KM (2008) Surface interactions and quantum kinetic molecular sieving for H₂ and D₂ adsorption on a mixed metal-organic framework material. *J Am Chem Soc* 130:6411–6423

64. Makowski P, Thomas A, Kuhn P, Goettmann F (2009) Organic materials for hydrogen storage applications: from physisorption on organic solids to chemisorption in organic molecules. *Energy Environ Sci* 2:480–490
65. McKeown NB, Budd PM (2006) Polymers of intrinsic microporosity (PIMs): organic materials for membrane separations, heterogeneous catalysis and hydrogen storage. *Chem Soc Rev* 35:675–683
66. Budd PM, Butler A, Selbie J, Mahmood K, McKeown NB, Ghanem B, Msayib K, Book D, Walton A (2007) The potential of organic polymer-based hydrogen storage materials. *Phys Chem Chem Phys* 9:1802–1808
67. Tsyurupa MP, Davankov VA (2006) Porous structure of hypercrosslinked polystyrene: state-of-the-art mini-review. *React Funct Polym* 66(7):768–779
68. Wood CD, Tan B, Trewin A, Niu H, Bradshaw D, Rosseinsky MJ, Khimyak YZ, Campbell NL, Kirk R, Stöckel E, Cooper AI (2007) Hydrogen storage in microporous hypercrosslinked organic polymer networks. *Chem Mater* 19:2034–2048
69. Han SS, Furukawa H, Yaghi OM, Goddard WA (2008) Covalent organic frameworks as exceptional hydrogen storage materials. *J Am Chem Soc* 130:11580–11581
70. Furukawa H, Yaghi OM (2009) Storage of hydrogen, methane, and carbon dioxide in highly porous covalent organic frameworks for clean energy applications. *J Am Chem Soc* 131:8875–8883
71. El-Kaderi HM, Hunt JR, Mendoza-Cortés JL, Côté AP, Taylor RE, O’Keefe M, Yaghi OM (2007) Designed synthesis of 3D covalent organic frameworks. *Science* 316:268–272
72. Spoto G, Vitillo JG, Cocina D, Damin A, Bonino F, Zecchina A (2007) FTIR spectroscopy and thermodynamics of hydrogen adsorbed in a cross-linked polymer. *Phys Chem Chem Phys* 9:4992–4999
73. Comotti A, Bracco S, Distefano G, Sozzani P (2009) Methane, carbon dioxide and hydrogen storage in nanoporous dipeptide-based materials. *Chem Commun* 284–286
74. Msayib KJ, Book D, Budd PM, Chaukura N, Harris KDM, Helliwell M, Tedds S, Walton A, Warren JE, Xu M, McKeown NB (2009) Nitrogen and hydrogen adsorption by an organic microporous crystal. *Angew Chem Int Ed* 48:3273–3277
75. Panella B, Kossykh L, Dettlaff-Weglikowska U, Hirscher M, Zerbi G, Roth S (2005) Volumetric measurement of hydrogen storage in HCL-treated polyaniline and polypyrrole. *Synth Met* 151:208–210
76. Rose M, Böhlmann W, Sabo M, Kaskel S (2008) Element-organic frameworks with high permanent porosity. *Chem Commun* 2462–2464
77. Graham T (1866) On the absorption and dialytic separation of gases by colloid septa. *Philos Trans R Soc Lond* 156:399–439
78. Sandrock G, Suda S, Schlappbach L (1992) Applications. In: Schlappbach L (ed) Topics in applied physics vol. 67: hydrogen in intermetallic compounds II. Surface and dynamic properties, applications. Springer-Verlag, Berlin
79. Bowman RC Jr, Fultz B (2002) Metallic hydrides I: hydrogen storage and other gas-phase applications. *MRS Bull* 27(9):688–693
80. Sandrock G, Bowman RC Jr (2003) Gas-based hydride applications: recent progress and future needs. *J Alloy Compd* 356, 357:794–799
81. Fukai Y (2005) The metal-hydrogen system. Basic bulk properties, 2nd edn. Springer, Berlin
82. Alefeld G, Völkl J (eds) (1978) Topics in applied physics vol. 28: hydrogen in metals I. Basic properties. Springer-Verlag, Berlin
83. Alefeld G, Völkl J (eds) (1978) Topics in applied physics vol. 29: hydrogen in metals II. Application-oriented properties. Springer-Verlag, Berlin
84. Schlappbach L (ed) (1988) Topics in applied physics Vol. 63: hydrogen in intermetallic compounds I. Electronic, thermodynamic and crystallographic properties, preparation. Springer-Verlag, Berlin
85. Schlappbach L (ed) (1992) Topics in applied physics vol. 67: hydrogen in intermetallic compounds II. Surface and dynamic properties, applications. Springer-Verlag, Berlin

86. Wipf H (ed) (1997) Topics in applied physics vol. 73: hydrogen in metals III. Properties and applications. Springer-Verlag, Berlin
87. Sandrock G (1999) A panoramic overview of hydrogen storage alloys from a gas reaction point of view. *J Alloy Compd* 293–295:877–888
88. Libowitz GG, Hayes HF, Gibb TRP Jr (1958) The system zirconium-nickel and hydrogen. *J Phys Chem* 62(1):76–79
89. Reilly JJ, Wiswall RH (1967) The reaction of hydrogen with alloys of magnesium and copper. *Inorg Chem* 6(12):2220–2223
90. Reilly JJ, Wiswall RH (1968) The reaction of hydrogen with alloys of magnesium and nickel and the formation of Mg_2NiH_4 . *Inorg Chem* 7(11):2254–2256
91. van Vucht JHN, Kuijpers FA, Bruning HCAM (1970) Reversible room-temperature absorption of large quantities of hydrogen by intermetallic compounds. *Philips Res Rep* 25(2):133–140
92. Griessen R, Riesters T (1988) Heat of formation models. In: Schlapbach L (ed) Topics in applied physics vol. 67: hydrogen in intermetallic compounds I. Surface and dynamic properties, applications. Springer-Verlag, Berlin
93. Buschow KHJ, Bouten PCP, Miedema AR (1982) Hydrides formed from intermetallic compounds of two transition metals: a special class of ternary alloys. *Rep Prog Phys* 45:937–1039
94. Griessen R, Driessen A (1984) Heat of formation and band structure of binary and ternary metal hydrides. *Phys Rev B* 30(8):4372–4381
95. Yvon K (2003) Hydrogen in novel solid-state metal hydrides. *Z Kristallogr* 218:108–116
96. Luo S, Clewley JD, Flanagan TB, Bowman RC Jr, Wade LA (1998) Further studies of the isotherms of $\text{LaNi}_{5-x}\text{Sn}_x\text{-H}$ for $x = 0\text{--}0.5$. *J Alloy Compd* 267:171–181
97. Bowman RC Jr, Luo CH, Ahn CC, Witham CK, Fultz B (1995) The effect of tin on the degradation of $\text{LaNi}_{5-y}\text{Sn}_y$ metal hydrides during thermal cycling. *J Alloy Compd* 217:185–192
98. Chandra D, Reilly JJ, Chellappa R (2006) Metal hydrides for vehicular applications: the state of the art. *JOM* 58(2):26–32
99. Ivey DG, Northwood DO (2003) Storing energy in metal hydrides: a review of the physical metallurgy. *J Mater Sci* 18:321–347
100. Sandrock G, Thomas G (2001) The IEA/DOE/SNL on-line hydride databases. *Appl Phys A* 72:153–155
101. Feng F, Geng M, Northwood DO (2001) Electrochemical behaviour of intermetallic-based metal hydrides used in Ni/metal hydride (MH) batteries: a review. *Int J Hydrogen Energy* 26:725–734
102. Young K, Fetcenko MA, Li F, Ouchi T (2008) Structural, thermodynamic, and electrochemical properties of $\text{Ti}_x\text{Zr}_{1-x}(\text{VNiCrMnCoAl})_2$ C14 Laves phase alloys. *J Alloy Compd* 464:238–247
103. Luo W, Clewley JD, Flanagan TB, Oates WA (1992) Thermodynamic characterization of the Zr-Mn-H system Part 1. Reaction of H_2 with single-phase ZrMn_{2+x} C-14 Laves phase alloys. *J Alloy Compd* 185:321–338
104. Töpler J, Feucht K (1989) Results of a test fleet with metal hydride motor cars. *Z Phys Chem NF* 164:1451–1461
105. Reilly JJ, Wiswall RH (1974) Formation and properties of iron titanium hydride. *Inorg Chem* 13(1):218–222
106. Sakintuna B, Lamari-Darkrim F, Hirscher M (2007) Metal hydride materials for solid hydrogen storage: a review. *Int J Hydrogen Energy* 32:1121–1140
107. Nomura K, Akiba E (1995) H_2 Absorbing-desorbing characterization of the Ti-V-Fe alloy system. *J Alloy Compd* 231:513–517
108. Cho S-W, Shim G, Choi G-S, Park C-N, Yoo J-H, Choi J (2007) Hydrogen absorption-desorption properties of $\text{Ti}_{0.32}\text{Cr}_{0.43}\text{V}_{0.25}$ alloy. *J Alloy Compd* 430:136–141
109. Seo C-Y, Kim J-H, Lee PS, Lee J-Y (2003) Hydrogen storage properties of vanadium-based b.c.c solid solution metal hydrides. *J Alloy Compd* 348:252–257

110. Song XP, Pei P, Zhang PL, Chen GL (2008) The influence of alloy elements on the hydrogen storage properties in vanadium-based solid solution alloys. *J Alloy Compd* 455:392–397
111. Mazzolai G, Coluzzi B, Biscarini A, Mazzolai FM, Tuissi A, Agresti F, Lo Russo S, Maddalena A, Palade P, Principi G (2008) Hydrogen-storage capacities and H diffusion in bcc TiVCr alloys. *J Alloy Compd* 466:133–139
112. Wang J-Y (2009) Comparison of hydrogen storage properties of $\text{Ti}_{0.37}\text{V}_{0.38}\text{Mn}_{0.25}$ alloys prepared by mechanical alloying and vacuum arc melting. *Int J Hydrogen Energy* 34:3771–3777
113. Akiba E, Okada M (2002) Metallic hydrides III: body-centered-cubic solid-solution alloys. *MRS Bull* 27(9):699–703
114. Graetz J, Reilly JJ (2007) Kinetically stabilized hydrogen storage materials. *Scr Mater* 56:835–839
115. Hauback BC (2008) Structures of aluminium-based light weight hydrides. *Z Kristallogr* 223:636–648
116. Graetz J (2009) New approaches to hydrogen storage. *Chem Soc Rev* 38:73–82
117. Kuji T, Matsumura Y, Uchida H, Aizawa T (2002) Hydrogen absorption of nanocrystalline palladium. *J Alloy Compd* 330–332:718–722
118. Suleiman M, Jisrawi NM, Dankert O, Reetz MT, Bähz C, Kirchheim R, Pundt A (2003) Phase transition and lattice expansion during hydrogen loading of nanometer sized palladium clusters. *J Alloy Compd* 356–357:644–648
119. Pundt A (2004) Hydrogen in nano-sized metals. *Adv Eng Mater* 6(1–2):11–21
120. Pundt A, Kirchheim R (2006) Hydrogen in metals: microstructural aspects. *Annu Rev Mater Res* 36:555–608
121. Yamauchi M, Kobayashi H, Kitagawa H (2009) Hydrogen storage mediated by Pd and Pt nanoparticles. *ChemPhysChem* 10:2566–2576
122. Stampfer JF Jr, Holley CE Jr, Suttle JF (1960) The magnesium-hydrogen system. *J Am Chem Soc* 82(14):3504–3508
123. Huot J, Liang G, Schulz R (2001) Mechanically alloyed metal hydride systems. *Appl Phys A* 72:187–195
124. Corey RL, Ivancic TM, Shane DT, Carl EA, Bowman RC Jr, Bellosa von Colbe JM, Dornheim M, Bormann R, Huot J, Zidan R, Stowe AC, Conradi MS (2008) Hydrogen motion in magnesium hydride by NMR. *J Phys Chem C* 112:19784–19790
125. Zaluska A, Zaluski L, Ström-Olsen JO (2001) Structure, catalysis, and atomic reactions on the nano-scale: a systematic approach to metal hydrides for hydrogen storage. *Appl Phys A* 72:157–165
126. Gross AF, Ahn CC, Van Atta SL, Liu P, Vajo JJ (2009) Fabrication and hydrogen sorption behaviour of nanoparticulate MgH_2 incorporated in a porous carbon host. *Nanotechnology* 20:204005
127. Aguey-Zinsou K-F, Ares-Fernández J-R (2008) Synthesis of colloidal magnesium: a near room temperature store for hydrogen. *Chem Mater* 20:376–378
128. Barkhordarian G, Klassen T, Bormann R (2006) Catalytic mechanism of transition-metal compounds on Mg hydrogen sorption reaction. *J Phys Chem* 110:11020–11024
129. Aguey-Zinsou K-F, Ares Fernandez JR, Klassen T, Bormann R (2007) Effect of Nb_2O_5 on MgH_2 properties during mechanical milling. *Int J Hydrogen Energy* 32:2400–2407
130. Wagemans RWP, van Lenthe JH, de Jongh PE, van Dillen AJ, de Jong KP (2005) Hydrogen storage in magnesium clusters: quantum chemical study. *J Am Chem Soc* 127:16675–16680
131. Grant D (2008) Magnesium hydride for hydrogen storage. In: Walker G (ed) *Solid-state hydrogen storage: materials and chemistry*. Woodhead Publishing, Cambridge
132. Suryanarayana C (2001) Mechanical alloying and milling. *Prog Mater Sci* 46:1–184
133. Suryanarayana C, Koch CC (2000) Nanocrystalline materials—current research and future directions. *Hyperfine Interact* 130:5–44
134. Suryanarayana C (2002) The structure and properties of nanocrystalline materials: issues and concerns. *JOM* 54(9):24–27

135. Bérubé V, Radtke G, Dresselhaus M, Chen G (2007) Size effects on the hydrogen storage properties of nanostructured metal hydrides: a review. *Int J Energy Res* 31:637–663
136. Maeland AJ, Tanner LE, Libowitz GG (1980) Hydrides of metallic glass alloys. *J Less-Common Met* 74:279–285
137. Orimo S, Fujii H (1998) Effects of nanometer-scale structure on hydriding properties of Mg-Ni alloys: a review. *Intermetallics* 6:185–192
138. Zaluski L, Zaluska A, Tessier P, Ström-Olsen JO, Schulz R (1995) Effects of relaxation on hydrogen absorption in Fe-Ti produced by ball-milling. *J Alloy Compd* 227:53–57
139. Bououdina M, Fruchart D, Jacquet S, Pontonnier L, Soubeyrou JL (1999) Effect of nickel alloying by using ball milling on the absorption properties of TiFe. *Int J Hydrogen Energy* 24:885–890
140. Harris JH, Curtin WA, Schultz L (1988) Hydrogen storage characteristics of mechanically alloyed amorphous metals. *J Mater Res* 3(5):872–883
141. Liang G, Huot J, Schulz R (2001) Hydrogen storage properties of the mechanically alloyed LaNi_5 -based materials. *J Alloy Compd* 320:133–139
142. Hotta H, Abe M, Kuji T, Uchida H (2007) Synthesis of Ti-Fe alloys by mechanical alloying. *J Alloy Compd* 439:221–226
143. Abe M, Kuji T (2007) Hydrogen absorption of TiFe alloy synthesized by ball milling and post-annealing. *J Alloy Compd* 446–447:200–203
144. Huot J, Enoki H, Akiba E (2008) Synthesis, phase transformation, and hydrogen storage properties of ball-milled $\text{TiV}_{0.9}\text{Mn}_{1.1}$. *J Alloy Compd* 453:203–209
145. Parente A, Nale A, Catti M, Kopnin E, Caracino P (2008) Hydrogenation properties of Mg_2AlNi_2 and mechanical alloying in the Mg-Al-Ni system. *J Alloy Compd* 477(1–2): 420–424
146. Corré S, Bououdina M, Kuriyama N, Fruchart D, Adachi G (1999) Effects of mechanical grinding on the hydrogen storage and electrochemical properties of LaNi_5 . *J Alloy Compd* 292:166–173
147. Fujii H, Munehiro S, Fujii K, Orimo S (2002) Effect of mechanical grinding under Ar and H_2 atmospheres on structural and hydriding properties in LaNi_5 . *J Alloy Compd* 330–332:747–751
148. Ares JR, Cuevas F, Percheron-Guégan A (2004) Influence of thermal annealing on the hydrogenation properties of mechanically milled AB_5 -type alloys. *Mater Sci Eng B* 108:76–80
149. Singh A, Singh BK, Davidson DJ, Srivastava ON (2004) Studies on improvement of hydrogen storage capacity of AB_5 type: $\text{MmNi}_{4.6}\text{Fe}_{0.4}$ alloy. *Int J Hydrogen Energy* 29:1151–1156
150. Takeichi N, Senoh H, Takeshita HT, Oishi T, Tanaka H, Kiyobayashi T, Kuriyama N (2004) Hydrogenation properties and structure of Ti-Cr alloy prepared by mechanical grinding. *Mater Sci Eng B* 108:100–104
151. Santos SF, Costa ALM, de Castro JFR, dos Santos DS, Botta WJ, Ishikawa TT (2004) Mechanical and reactive milling of a TiCrV BCC solid solution. *J Metastable Nanocrystalline Mater* 20–21:291–296
152. Singh BK, Shim G, Cho S-W (2007) Effects of mechanical milling on hydrogen storage properties of $\text{Ti}_{0.32}\text{Cr}_{0.43}\text{V}_{0.25}$ alloy. *Int J Hydrogen Energy* 32:4961–4965
153. Orimo S, Züttel A, Ikeda K, Saruki S, Fukunaga T, Fujii H, Schlapbach L (1999) Hydriding properties of the MgNi-based systems. *J Alloy Compd* 293–295:437–442
154. Terashita N, Takahashi M, Kobayashi K, Sasai T, Akiba E (1999) Synthesis and hydriding/dehydriding properties of amorphous $\text{Mg}_2\text{Ni}_{1.9}\text{M}_{0.1}$ alloys mechanically alloyed from $\text{Mg}_2\text{Ni}_{0.9}\text{M}_{0.1}$ (M = none, Ni, Ca, La, Y, Al, Si, Cu and Mn) and Ni powder. *J Alloy Compd* 293–295:541–545
155. Varin RA, Czujko T, Wronski ZS (2009) *Nanomaterials for solid state hydrogen storage*. Springer, New York
156. Bowman RC Jr (1988) Preparation and properties of amorphous hydrides. *Mater Sci Forum* 31:197–228

157. Eliaz N, Eliezer D (1999) An overview of hydrogen interaction with amorphous alloys. *Adv Perform Mater* 6:5–31
158. Shechtman D, Blech I, Gratias D, Cahn JW (1984) Metallic phase with long-range orientational order and no translational symmetry. *Phys Rev Lett* 53(20):1951–1953
159. Tsai AP (2008) Icosahedral clusters, icosahedral order and stability of quasicrystals - a view of metallurgy. *Sci Technol Adv Mater* 9:013008
160. Bindi L, Steinhardt PJ, Yao N, Lu PJ (2009) Natural quasicrystals. *Science* 324:1306–1309
161. Takasaki A, Kelton KF (2002) High-pressure hydrogen loading in $\text{Ti}_{45}\text{Zr}_{38}\text{Ni}_{17}$ amorphous and quasicrystal powders synthesized by mechanical alloying. *J Alloy Compd* 347:295–300
162. Takasaki A, Kelton KF (2006) Hydrogen storage in Ti-based quasicrystal powders produced by mechanical alloying. *Int J Hydrogen Energy* 31:183–190
163. Bystrzycki J, Polanski M, Malka IE, Komuda A (2009) Hydriding properties of Mg-Al-Zn quasicrystal powder produced by mechanical alloying. *Z Kristallogr* 224:105–108
164. Bogdanović B, Schwickardi M (1997) Ti-doped alkali metal aluminium hydrides as potential novel reversible hydrogen storage materials. *J Alloy Compd* 253–254:1–9
165. Chen P, Xiong Z, Luo J, Lin J, Tan KL (2002) Interaction of hydrogen with metal nitrides and imides. *Nature* 420:302–304
166. Schüth F, Bogdanović B, Felderhoff M (2004) Light metal hydrides and complex hydrides for hydrogen storage. *Chem Commun* 2249–2258
167. Orimo S, Nakamori Y, Eliseo JR, Züttel A, Jensen CM (2007) Complex hydrides for hydrogen storage. *Chem Rev* 107:4111–4132
168. Jensen C, Yang Y, Chou MY (2008) Alanates as hydrogen storage materials. In: Walker G (ed) *Solid-state hydrogen storage: materials and chemistry*. Woodhead Publishing, Cambridge
169. Jensen CM, Zidan R, Mariels N, Hee A, Hagen C (1999) Advanced titanium doping of sodium aluminium hydride: segue to a practical hydrogen storage material? *Int J Hydrogen Energy* 24:461–465
170. Zidan RA, Takara S, Hee AG, Jensen CM (1999) Hydrogen cycling behavior of zirconium and titanium-zirconium-doped sodium aluminium hydride. *J Alloy Compd* 285:119–122
171. Bogdanović B, Felderhoff M, Pommerin A, Schüth F, Spielkamp N (2006) Advanced hydrogen-storage materials based on Sc-, Ce-, and Pr-doped NaAlH_4 . *Adv Mater* 18:1198–1201
172. Jensen CM, Gross KJ (2001) Development of catalytically enhanced sodium aluminium hydride as a hydrogen-storage material. *Appl Phys A* 72:213–219
173. Eberle U, Felderhoff M, Schüth F (2009) Chemical and physical solutions for hydrogen storage. *Angew Chem Int Ed* 48:6608–6630
174. Lohstroh W, Fichtner M, Breitung W (2009) Complex hydrides as solid storage materials: first safety tests. *Int J Hydrogen Energy* 34:5981–5985
175. Graetz J, Lee Y, Reilly JJ, Park S, Vogt T (2005) Structures and thermodynamics of the mixed alkali alanates. *Phys Rev B* 71:184115
176. Léon A, Zabara O, Sartori S, Eigen N, Dornheim M, Klassen T, Muller J, Hauback B, Fichtner M (2009) Investigation of (Mg, Al, Li, H)-based hydride and alanate mixtures produced by reactive ball milling. *J Alloy Compd* 476:425–428
177. Sartori S, Léon A, Zabara O, Muller J, Fichtner M, Hauback BC (2009) Studies of mixed hydrides based on Mg and Ca by reactive ball milling. *J Alloy Compd* 476:639–643
178. Sartori S, Qi X, Eigen N, Muller J, Klassen T, Dornheim M, Hauback BC (2009) A search for new Mg- and K-containing alanates for hydrogen storage. *Int J Hydrogen Energy* 34:4582–4586
179. Gregory DH (2008) Lithium nitrides, imides and amides as lightweight, reversible hydrogen stores. *J Mater Chem* 18:2321–2330
180. Hino S, Ichikawa T, Ogita N, Udagawa M, Fujii H (2005) Quantitative estimation of NH_3 partial pressure in H_2 desorbed from the Li-N-H system by Raman spectroscopy. *Chem Commun* 3038–3040

181. Uribe FA, Gottesfeld S, Zawodzinski TA Jr (2002) Effect of ammonia as potential fuel impurity on proton exchange membrane fuel cell performance. *J Electrochem Soc* 149(3):A293–A296
182. Gregory DH (2008) Imides and amides as hydrogen storage materials. In: Walker G (ed) *Solid-state hydrogen storage: materials and chemistry*. Woodhead Publishing, Cambridge
183. Züttel A, Rentsch S, Fischer P, Wenger P, Sudan Mauron P, Emmenegger C (2003) Hydrogen storage properties of LiBH_4 . *J Alloy Compd* 356–357:515–520
184. Nakamori Y, Orimo S (2008) Borohydrides as hydrogen storage materials. In: Walker G (ed) *Solid-state hydrogen storage: materials and chemistry*. Woodhead Publishing, Cambridge
185. Walker G (2008) Multicomponent hydrogen storage systems. In: Walker G (ed) *Solid-state hydrogen storage: materials and chemistry*. Woodhead Publishing, Cambridge
186. Orimo S, Fujii H (2001) Materials science of Mg-Ni-based new hydrides. *Appl Phys A* 72:167–186
187. Blomqvist H, Rönnebro E, Noréus D, Kujii T (2002) Competing stabilisation mechanisms in Mg_2NiH_4 . *J Alloy Compd* 330–332:268–270
188. Häussermann U, Blomqvist H, Noréus D (2002) Bonding and stability of the hydrogen storage material Mg_2NiH_4 . *Inorg Chem* 41:3684–3692
189. Mao WL, Koh CA, Sloan ED (2007) Clathrate hydrates under pressure. *Phys Today* 60(10):42–47
190. Mao WL, Mao H, Goncharov AF, Struzhkin VV, Guo Q, Hu J, Shu J, Hemley RJ, Somayazulu M, Zhao Y (2002) Hydrogen clusters in clathrate hydrate. *Science* 297:2247–2249
191. Struzhkin VV, Militzer B, Mao WL, Mao HK, Hemley RJ (2007) Hydrogen storage in molecular clathrates. *Chem Rev* 107:4133–4151
192. Florusse LJ, Peters CJ, Schoonman J, Hester KC, Koh CA, Dec SF, Marsh KN, Sloan ED (2004) Stable low-pressure hydrogen clusters stored in a binary clathrate hydrate. *Science* 306:469–471
193. Lee H, Lee J, Kim DY, Park J, Seo Y-T, Zeng H, Moudrakovski IL, Ratcliffe CI, Ripmeester JA (2005) Tuning clathrate hydrates for hydrogen storage. *Nature* 434:743–746
194. Papadimitriou NI, Tsimpanogiannis IN, Papaioannou AT, Stubos AK (2008) Evaluation of the hydrogen-storage capacity of pure H_2 and binary H_2 -THF hydrates with Monte Carlo simulations. *J Phys Chem C* 112:10294–10302
195. Papadimitriou NI, Tsimpanogiannis IN, Peters CJ, Papaioannou AT, Stubos AK (2008) Hydrogen storage in sH hydrates: a Monte Carlo study. *J Phys Chem B* 112:14206–14211
196. Duarte ARC, Shariati A, Rovetto LJ, Peters CJ (2008) Water cavities of sH clathrate hydrate stabilized by molecular hydrogen: phase equilibrium measurements. *J Phys Chem B* 112(7):1888–1889
197. Strobel TA, Koh CA, Sloan ED (2008) Water cavities of sH clathrate hydrate stabilized by molecular hydrogen. *J Phys Chem B* 112(7):1885–1887
198. Daschbach JL, Chang T-M, Corrales LR, Dang LX, McGrail P (2006) Molecular mechanisms of hydrogen-loaded β -hydroquinone clathrate. *J Phys Chem B* 110:17291–17295
199. Strobel TA, Kim Y, Andrews GS, Ferrell JR III, Koh CA, Herring AM, Sloan ED (2008) Chemical-clathrate hybrid hydrogen storage: storage in both guest and host. *J Am Chem Soc* 130:14975–14977
200. Yoon J-H, Lee Y-J, Park J, Kawamura T, Yamamoto Y, Komai T, Takeya S, Han SS, Lee J-W, Lee Y (2009) Hydrogen molecules trapped in interstitial host channels of α -hydroquinone. *ChemPhysChem* 10:352–355
201. Su F, Bray CL, Tan B, Cooper AI (2008) Rapid and reversible hydrogen storage in clathrate hydrates using emulsion-templated polymers. *Adv Mater* 20:2663–2666
202. Su F, Bray CL, Carter BO, Overend G, Cropper C, Iggo JA, Khimyak YZ, Fogg AM, Cooper AI (2009) Reversible hydrogen storage in hydrogel clathrate hydrates. *Adv Mater* 21:1–5

203. Plechkova NV, Seddon KR (2008) Applications of ionic liquids in the chemical industry. *Chem Soc Rev* 37:123–150
204. Olivier-Bourbigou H, Magna L, Morvan D (2010) Ionic liquids and catalysis: recent progress from knowledge to applications. *Appl Catal A* 373:1–56
205. Stracke MP, Ebeling G, Cataluña R, Dupont J (2007) Hydrogen-storage materials based on imidazolium ionic liquids. *Energy Fuels* 21:1695–1698
206. Wang L, Yang RT (2008) New sorbents for hydrogen storage by hydrogen spillover—a review. *Energy Environ Sci* 1:268–279
207. Cheng H, Chen L, Cooper AC, Sha X, Pez GP (2008) Hydrogen spillover in the context of hydrogen storage using solid-state materials. *Energy Environ Sci* 1:338–354
208. Conner WC, Falconer JL (1995) Spillover in heterogeneous catalysis. *Chem Rev* 95: 759–788
209. Lachawiec AJ, Qi G, Yang RT (2005) Hydrogen storage in nanostructured carbons by spillover: bridge-building enhancement. *Langmuir* 21:11418–11424
210. Rao CNR, Nath M (2003) Inorganic nanotubes. *Dalton Trans* 1–24
211. Seayad AM, Antonelli DM (2004) Recent advances in hydrogen storage in metal-containing inorganic nanostructures and related materials. *Adv Mater* 16(9–10):765–777
212. Ma R, Bando Y, Zhu H, Sato T, Xu C, Wu D (2002) Hydrogen uptake in boron nitride nanotubes at room temperature. *J Am Chem Soc* 124:7672–7673
213. Oku T, Kuno M, Narita I (2004) Hydrogen storage in boron nitride nanomaterials studied by TG/DTA and cluster calculation. *J Phys Chem Solids* 65:549–552
214. Chen J, Li S-L, Tao Z-L, Shen Y-T, Cui C-X (2003) Titanium disulfide nanotubes as hydrogen-storage materials. *J Am Chem Soc* 125:5284–5285
215. Chen J, Li SL, Tao ZL (2003) Novel hydrogen storage properties of MoS₂ nanotubes. *J Alloy Compd* 356–357:413–417
216. Tang C, Bando Y, Ding X, Qi S, Golberg D (2002) Catalyzed collapse and enhanced hydrogen storage of BN nanotubes. *J Am Chem Soc* 124(49):14550–14551
217. Bavykin DV, Lapkin AA, Plucinski PK, Friedrich JM, Walsh FC (2005) Reversible storage of molecular hydrogen by sorption into multilayered TiO₂ nanotubes. *J Phys Chem B* 109:19422–19427
218. Pan H, Feng YP, Lin J (2007) Hydrogen adsorption by tungsten carbide nanotube. *Appl Phys Lett* 90:223104
219. Lan J, Cheng D, Cao D, Wang W (2008) Silicon nanotube as a promising candidate for hydrogen storage: from the first principle calculations to Grand Canonical Monte Carlo simulations. *J Phys Chem C* 112:5598–5604
220. Mpourmpakis G, Froudakis GE, Lithoxoos GP, Samios J (2006) SiC nanotubes: a novel material for hydrogen storage. *Nano Lett* 6(8):1581–1583
221. Binewale RB, Rayalu S, Devotta S, Ichikawa M (2008) Chemical hydrides: a solution to high capacity hydrogen storage and supply. *Int J Hydrogen Energy* 33:360–365
222. Christensen CH, Johannessen T, Sørensen RZ, Nørskov JK (2006) Towards an ammonia-mediated hydrogen economy? *Catal Today* 111:140–144
223. Wiswall R (1978) Hydrogen storage in metals. In: Alefeld G, Völkl J (eds) *Topics in applied physics vol. 29: hydrogen in metals II. Application-oriented properties*. Springer-Verlag, Berlin
224. Bull DJ, Weidner E, Shabalin IL, Telling MTF, Jewell CM, Gregory DH, Ross DK (2010) Pressure-dependent deuterium reaction pathways in the Li-N-D system. *Phys Chem Chem Phys* 12:2089–2097
225. Lemmon EW, Huber ML, McLinden MO (2007) NIST standard reference database 23: reference fluid thermodynamic and transport properties-REFPROP, version 8.0, National Institute of Standards and Technology, Standard Reference Data Program, Gaithersburg
226. Hodoshima S, Arai H, Saito Y (2003) Liquid-film-type catalytic decalin dehydrogenation for long-term storage and long-distance transportation of hydrogen. *Int J Hydrogen Energy* 28:197–204

Hydrogen Storage Materials

The Characterisation of Their Storage Properties

Broom, D.P.

2011, XII, 260 p., Hardcover

ISBN: 978-0-85729-220-9